Florida Water Resources Research Center
Annual Technical Report
FY 2005

Introduction

The mission of the WRRC is to serve as a center of expertise in the water resources field, assist public and private interests in the conservation, development, and use of water resources, provide opportunities for professional training, assist local, state, regional, and federal agencies in planning and regulation, and communicate research findings to interested users. The WRRC administers funding received from the federal Water Resources Research Act of 1984 and coordinates water-resources research and technology transfer as authorized by the funding, acts as liaison for Florida Agencies and water management districts, promotes water-resources research by seeking external support, and seeks to enhance the state and national image of the University of Florida (UF) as a focal point for water resources research. The WRRC is funded in part by Section 104 of Public Law 98-42 and Public Law 104-99, which are administered by the U.S. Geological Survey, Department of the Interior. Additional funding and support are provided by UF and research sponsors that include state agencies such as the water management districts.

Research Program

During FY 2005, the Florida Water Resources Research Center (WRRC) supported three research projects. Two of the projects were supported by funds through the 104B program, and one project was a continuation of work funded through the 104G program from FY 2004. In the first 104B project, work was performed to develop an integrated methodology to assess the vulnerability of ground water to pathogen intrusion using GIS, remote sensing, neural networks and neuro-fuzzy methods. The second 104B project investigated mechanisms and modeling of soft-bed nutrient release in lakes. In the 104G project, space-based observations are being used to understand the complexity of wetland surface flow in order to better manage wetlands and water resources.

Development of an integrated methodology to assess vulnerability of groundwater to pathogen intrusion using GIS, remote sensing, neural networks and neuro-fuzzy methods

Basic Information

Title:	Development of an integrated methodology to assess vulnerability of groundwater to pathogen intrusion using GIS, remote sensing, neural networks and neuro-fuzzy methods
Project Number:	2005FL100B
Start Date:	3/1/2005
End Date:	2/28/2006
Funding Source:	104B
Congressional District:	10th
Research Category:	Ground-water Flow and Transport
Focus Category:	Models, Management and Planning, Groundwater
Descriptors:	
Principal Investigators:	Barnali Dixon

Publication

1. Dixon, B, Candade, N. and Julie Earls. 2006. Development of an integrated methodology to assess vulnerability of ground water to pathogen intrusion using GIS, remote sensing, neural networks and neuro-fuzzy methods. American Association of Geographers, Annual Meeting, Chicago, IL, March.
2. Dixon, B. and Candade N. 2005. Integrated GIS and machine learning algorithms applied to ground water contamination mapping: a comparative study. Applied Geography Conference. Washington D.C. November.
3. Dixon, B. and Candade N. 2005. Groundwater Contamination Mapping Using Integrated GIS and Neural Networks: A Sensitivity Analysis. Presentation. International Conference on Environmental Science and Technology. January, New Orleans.
4. Candade, N. and B. Dixon. 2005. Effects of Training Sizes and Dimensionality on NN and SVM Performance: A Comparative Study. American Association of Geographers, Annual Meeting, Denver, CO, April.

Development of an integrated methodology to assess vulnerability of ground water to pathogen intrusion using GIS, remote sensing, neural networks and neuro-fuzzy methods

FINAL COMPLETION REPORT

Subcontract UF-EIES-0404012-USF (3/1/05 - 2/28/06)

PI: Barnali Dixon Ph.D.
University of South Florida St. Petersburg
Davis Hall 258
140 Seventh Ave South
St. Petersburg
FL 33701
Phone: 727 553 4025
Email: bdixon@stpt.usf.edu

COMPARISON OF NEURAL NETWORK AND NEURO-FUZZY TECHNIQUES IN GROUND WATER VULNERABILITY MAPPING: A CASE STUDY

Barnali Dixon[1]

1. INTRODUCTION

Contamination of surface and subsurface waters by anthropogenic activities has been a major concern of agencies involved with water management, water quality, water quantity and human health. Ground water (GW) accounts for 60% of the fresh water withdrawals in Florida and about 51% of this water is being used without further treatment or disinfection (Marella, 19999). Occurrence of well-drained sandy soils and karst features along with high rainfall makes Florida's GW, a major source of freshwater supply, vulnerable to contamination (Berndt et al, 1998; Purdum, 2002; Lee et. al, 2002). The proportion of outbreaks associated with groundwater sources in Florida increased 87% from the previous reporting period, and these outbreaks were primarily associated (60.7%) with consumption of untreated groundwater (Lee et. al, 2002). Close connection between ground and surface water, common in Florida, means that pathogens found in surface water may find their way into GW and vice versa. In recent years, Florida has been one of the most common relocation destinations in the US. Florida's population grew from 4 million in 1955 to 16 million in 2000, the highest growth rate in the nation. As a result, we have two inevitable problems throughout Florida i) increased amount of wastewater treatment and resultant sludge production, and (ii) increased number (and density) of septic systems. One of the dominant ways of sludge disposal is land application. Florida Department of health (FLDEP) has established detailed regulations for processing sludge before application and controlling the application of sludge to land. In 2003, 66% of the sludge was land applied in Florida, 17% were land-filled, and remaining 17% accounted for distribution and marketing. (http://www.dep.state.fl.us/water/wastewater/dom/reshome.htm). In Florida, parks and golf courses are common sites for Class A sludge application whereas many farmers apply Class B sludge to their pasture and farmland to reduce cost of fertilizer and lime. Since most processes used for complete pathogen/viral inactivation is not sufficient (EPA, 2003), landowners and the public as well as regulatory agencies are justifiably concerned about potential negative impacts of the potential spread of pathogens and resultant outbreaks. Therefore, there is a need to adopt waste application practices that take into consideration soil properties, hydrogeology, hydraulic loading and contaminant transport characteristics to minimize pathogen contamination risk (EPA, 2003). Additionally, in Florida, 31% of the population is served by estimated 2.3 million septic systems. These systems discharge over 426 million gallons of waste water per day into the subsurface soil environment (Florida Dept. of Health (DOH) http://www.doh.state.fl.us/environment/OSTDS/intro.html). Inadequately treated sewage from septic systems can lead to contamination of groundwater and poses a significant threat to drinking water and human health (http://www.epa.gov/owm/septic/pubs/homeowner_guide_long.pdf). There are no easy solutions to the sludge disposal or septic tank problems in Florida.

Traditionally state and county regulators used fixed setback distances for sludge application and septic tank locations for all geologic setting in their jurisdiction to protect our water resources (EPA, 2003). One approach in determining setback is to the use travel time using GW flow characteristics (Yeats and Yeats, 1987). A comprehensive study conducted by Matthesss et al (1984) that used the aforementioned approach showed that ground water flow-based 50 day residence time was not adequate for all of the sites for virus reduction. It takes longer and varied between 160 days and 270 days (EPA, 2003). Study conducted for Ground Water Rule showed that setback distances were found to be quite variable (EPA, 2000). Some distances were scientific and others

---

[1] Assistant Professor, University of South Florida, St. Petersburg. 140 seventh ave south, St. Petersburg, Fl 33701. Phone: 727 553 4025, bdixon@stpt.usf.edu

were holdovers from past practices (EPA, 2003). Very few of them considered preferential flow paths common in Florida karst. A table summarized by EPA (2003) listed critical factors that control pathogen/viral transport. They are: soil moisture content, type and depth of the soils, soil porperties such as organic matter and pH as well as hydraulic conditions to name a few. It is obvious that these factors vary over the landscape. Therefore, one size fits all mode of regulations for establishing setback distances might not be adequate. Conducting site- specific studies (on a case by case basis) to regulate entire Florida will clearly be cost prohibitive. Therefore, there is a need to strike a balance between expensive site-specific studies and broad-based one-size fits all policy. We are proposing to develop a spatially explicit method that will provide a vulnerability map for an area based on similar hydrogeological, topographical, climatological, soils, preferential flow pathways and landuse. This will be a useful environmental management tool to establish setback rules. This vulnerability map will have explicit representation of the possible level of risk associated with GW vulnerability to pathogens. In a gross sense, information from soil surveys, hydrologeological parameters, and landuse will be incorporated in a screening tool that will provide an indication of the level of risk a particular site may have to GW contamination by pathogen.

Coupling of neural networks (NN) and neuro-fuzzy models with a Geographic Information System (GIS) will facilitate vulnerability mapping of a complex system with enhanced spatial visualization capabilities of the models as suggested by Burrough (1996), Corwin et al., (1996). Integration with GIS will allow us to evaluate sensitivity of NN and neuro-fuzzy in a spatial context.

NN are multi-input, multi-output nonlinear models and can represent the complex interactions among the input/output parameters. In recent years NN has been successfully used in solving difficult hydrological and environmental problems. One major criticism is that it is not possible to determine how the solution was found due to the inherent black box nature of the NN. Also, it is also not possible to insert prior knowledge to a NN. The question is does NN need prior knowledge?? Also, how sensitive NNs are??

Incorporation of fuzzy logic with a GIS has shown to reduce error propagation (Wang et, al, 1990; Burrough et al 1992; De Gruizter, et al. 1997). Neuro-fuzzy modeling is an approach where the fusion of NN and Fuzzy Logic find their strengths and complement each other (Dixon, 2001, 2002, Khan, 1999, Nauck and Kruse, 1999). A key disadvantage of fuzzy logic based approach is inability to meet pre specified accuracy and lack of self-learning and generalization capability.

Neuro-fuzzy approach employs heuristic learning strategies derived from the domain of NN theory to support the development of a fuzzy system. A marriage between NN and fuzzy logic techniques should help overcome the shortcomings of both techniques discussed at length by Nauck and Kruse (1999). A neuro-fuzzy technique can learn a system's behavior from a sufficiently large data set and automatically generate fuzzy rules and fuzzy sets to a pre-specified accuracy level. They are capable of generalization, thus overcoming to the key disadvantages of fuzzy logic based approach. A fusion of NN and fuzzy logic provides a system that usually requires less computational power but has the ability to generalize and learn through the convergence of net. The research reports a case study of Polk County, Florida. This County was selected for its extensive agricultural landuse and the presence of underlying alluvial aquifer. This study aimed at using selected parameters from the DRASTIC model (Aller et al.,) with the NN and Neuro-fuzzy. Authors are aware of the strength and weaknesses of the DRASTIC model. The authors used parameters from the DRASTIC in this study because of readily available GIS layers for the Polk County. The intention of this study is not to promote or criticize DRASTIC.

2. OBJECTIVES

This study aims at comparing the vulnerability maps developed using NN and neuro-fuzzy methods. Specific objectives are to: i) compare the NN models with neuro-fuzzy and (ii) to check the sensitivity of NN and neuro-fuzzy models to training data.

3. METHODOLOGY

3.1 Digital Database

The DRASTIC model (Aller et al, 1987) is comprised of seven hydro geological variables: Depth to ground water (D), Recharge of aquifer (R), Aquifer media (A), Soil media (S), Topography/slope (T), Impact of vadose zone (I) and hydraulic Conductivity (C). Only four out of these seven variables were used as inputs for both NN and Neuro-fuzzy models. A, T and C were not used in the models due to lack of variability. All seven parameters were derived from the primary data layers in a GIS. The primary data layers used in this study are potentiometric surface, elevation, soils and geology. All of these primary data layers except soils were obtained from US Geological Survey (USGS). The soils data were obtained from the Natural Resource Conservation Service (NRCS). Digital Elevation Models (DEMs) with 30m resolution were used to generate elevation data for the study area. Potentiometric surface data provided by USGS was collected during the fall of 1996. This data was recorded in contour line with 20 ft interval. Potentiometric surface was generated using the GRASS command s.surf.tps. The data layer for D was generated by subtracting potentiometric surface from elevation. The data layer for net recharge was obtained from USGS. The net recharge was calculated based on the past behavior of the aquifer using MODFLOW at a one square mile cell resolution. The output from the MODFLOW was a site file. The site file was interpolated in GRASS to create the data layer R. The data layer for S was created through a multi-step process. Soil leaching index and soil pesticide leaching potential data were used to create the layer S. Soil leaching index layer was obtained from annual precipitation and soil hydrologic group. Soil pesticide leaching potential was created from soil attenuation, soil infiltration and soil permeability data layers. Soil attenuation information was generated from GLEAMS model. Please refer to Smith et al. (1994) for details. Thickness of the clay cap (I) is an important property since it influences the recharge to the aquifer and pesticide adsorption and degradation processes. GRASS command s.surf.tps was performed on the point data provided by USGS to create the interpolated surface. SSURGO data were used create maps for bulk density (BD), soils drainage class (D), soil Hydrologic group (H) (referred together as DH), soils structure or pedality. Landuse data we obtained from SWFWMD (1999).

Water quality data from 55 wells were used for validation of the models. The water quality data was provided by the Florida Department of Environmental Protection (FLDEP) in an excel spreadsheet containg well ID with locations of wells collected using a Global Positioning System (GPS). GRASS command s.menu was used to create site files for the wells. The wells then were reclassed into 2 categories: contaminated wells and non-contaminated wells. Single occurrence of E Coli was considered as contaminated well. (See Appendix A) for summery..

3.2 Coupling of NN and Neuro-fuzzy with GIS

Table 1. Example of Training Data used with NEFCLASS-J.

Nefclass J inputs				Output vulnerability			
D	R	S	I	Low	Mod low	Moder ate	High
NF1							
3	1	1	5	1	0	0	0
7	3	9	7	0	0	1	0
7	1	5	8	0	0	0	1
9	1	2	5	0	1	0	0
NF2 & NF3							
63	1	1	35	1	0	0	0
23	3	9	15	0	0	1	0
23	1	5	10	0	0	0	1
10	1	2	35	0	1	0	0

Modeling of GW vulnerability was accomplished by loosely coupling GIS (GRASS 4.1) and NN software PREDICT (Neuralware, 2001, version 2.4) and the Neuro-fuzzy software Nefclass-J (Nauck and Kruse, 1999 version 1.0). The output function (single column n ASCII output) of NEFCLASS-J was modified to make files compatible with the GRASS. The NN software PREDICT has limitation of number of rows of data it can take. It can only take 132,000 of rows for each run. The application data for the Polk County consisted of 4,093,760 rows. So a custom code in VC++ was written to break down our application dataset in manageable size for the PREDICT. This custom software is available at the website:www.stpt.usf.edu/bdixon/gal/mainpage_final.html.

Table 2. Example of Training Data used with PREDICT.

NN inputs				Output
D	R	S	I	Vulnerability
NN1				
3	1	1	5	1 Low
7	3	9	7	3 Moderate
7	1	5	8	4 High
9	1	2	5	2 Moderately Low
NN2 & NN3				
63	1	1	35	1 Low
23	3	9	15	3 Moderate
23	1	5	10	4 High
10	1	2	35	2 Moderately Low

Use of NN and Neuro-fuzzy requires training data and application data. The training and application data for the NEFCLASS-J and PREDICT was obtained from the GIS. GRASS command r.stats was used to create training dataset. This GRASS command generated all possible combinations of D, R, S and I for the County. The training data consisted of 408 rows. Examples of training data are given in the Tables 1 and 2.

3.3 Development of Neural Network model

The Standard Back Propagation (SBP) architecture provided by PREDICT was used to perform classification. Figure 1 shows the Multi Layer Perceptron (MLP) network architecture. SBP is a method for training the MLP. It is a method for assigning responsibility for mismatches to each of the processing elements in the network; this is achieved by propagating the gradient of the objective function back through the network to the hidden units. Based on the degree of responsibility, the weights of each

Example: Depth to ground water   Recharge   Soil media

individual processing element are modified iteratively to improve the objective function.
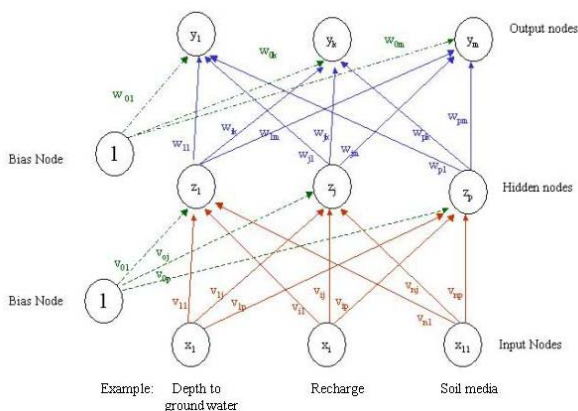
Use of NN is a 3-step process: i) training, ii) testing and iii) application. The entire training data was divided into 2 groups training (286) and testing (214) data sets. Once the NN was trained and tested, application data consisting of 4,093,760 rows were used to generate

ground water vulnerability maps. A batch file written in PREDICT automatically ran all the groups that were created, and produced the single column output. Examples of training parameter are presented in the Table 3.

Figure 1. Multi layer Perceptron Architecture

The training data for NN models was modified by adding a 0, 0, 0, 0 value to a total number of training pattern of 410. This was necessary because it was noted during simulation that an input of 0,0,0,0 in the application data resulted in a valid class of 1 (which indicates low vulnerability). But in reality these zero value represented data value out of the GIS mask but within the region. The following parameters were used with the PREDICT classifier:

Table 3: Parameters of NN Classifier

Learning Rate	Hidden layer=100
	Output layer=0.01
Learning Rule	Adaptive gradient
Variable selection model	Multiple regression
Training and testing	10-fold cross validation

The training data obtained from GRASS was inspected and classified based on expert's opinion according to the relationships between input parameter and the output vulnerability category. D and I are inversely related to the vulnerability categories whereas S and R are directly related. Examples of training rules are presented in the Table 4.

Table 4. Example of Rules used to Define Vulnerability.

D	(ft)	R	(inch/yr)	S	(rate)	I	(ft)	Output vulnerability categories [b]
				Inputs [a]				
Low	(0-5)	Low	(0-1)	Mod low	(mod slow)	Low	(11-20)	Moderate
Low		Low		High	(rapid)	Low		High
Low		Mod low	(5-7)	Low	(slow)	High	(51-75)	Moderately low
Low		Mod low		High		Low		High
High	(51-75)	Mod low		Mod low		Mod	(31-50)	Low
High		Mod	(8-10)	Mod low		Mod low	(21-30)	Moderate
High		High	(20)	High		Low		High
High		High		High		High		Moderate

a = inputs obtained from raster data layers

b = output vulnerability categories: manually classified based on expert's opinion.

3.4 Development of Neuro-fuzzy model

Neuro-fuzzy model also uses a supervised learning-like algorithm based on fuzzy error back propagation (Figure 2). The learning procedure for the fuzzy sets is a simple heuristics. It results in shifting the membership functions and in making their supports larger or smaller (Nauck and Kruse, 1999). The adaptation of fuzzy sets is carried out by simply changing the parameters of its membership function in a way that the membership degree for the current feature value is increased or decreased respectively.

In this research, the trapezoidal membership function was used since it was the most stable as compared to triangular and bell shaped membership functions (Dixon, 2001). The training parameter for the Neuro-fuzzy models are presented in the Table 5. Mathematically, trapezoidal membership function can be defined as follows:

$$(x : a, b, c, d) = \begin{cases} 0 & x < a \\ (x-a)/(b-a) & a <= x < b \\ 1 & b <= x < c \\ (d-x)/(d-c) & c <= x < d \\ 0 & x >= d \end{cases}$$

Figure 2: Neuro-Fuzzy architecture

For detailed description of membership functions and Neuro-fuzzy architecture please refer to Nauck and Kruse (1999). Use of Neuro-fuzzy model is also a 3-step process: i) training, ii) testing/validation and iii) application. The testing/validation technique used with the neuro-fuzzy model is 'cross validation'. This approach randomly divides the training data into the number of parts specified by the operator (10-fold for this project) and generalized errors are estimated from the results of the learning processes that are provided through a mean error and a confidence interval calculated at the 99% level. The same data that was used for training the NN was used here with the exception of two rows containing data value of 0,0,0,0. Thus the total number of patterns used for training was 408. NEFCLASS-J did not have problem in classifying data that were 0 (outside the GIS mask) as '0' category representing not classified category.

Table 5: Parameters of Neuro-fuzzy classifier

Learning Rate	0.01
No. of fuzzy sets	4 TRAPEZOIDAL for each variable
Rule learning strategy	Best per class
Stop control	Maximum number of epochs=1000
	Minimum number if epochs= 100
Validation mode	10-fold cross validation

3.5 Sensitivity Analysis

Sensitivity of the training data set was analyzed by changing the training data. A total of 26 models were created using neural networks and neuro-fuzzy methods ((13 per method). All models were compared to DRASTIC model too. First set of simulations was run using D, R, S and I value as reflected by the weight of the parameters outlined by the DRASTIC model. For details on weight of the parameters please refer to Dixon et al., (2002). These models from here on will be referred to as NN1, NN2 and so on for neural netweoks models and NF1, NF2 and so on for neuro fuzzy based models (Table 6).

7

Table 6. Summary of Model Parameters and Model Names

Models	Neural networks	Neuro-fuzzy	Name of Model
Model-1	NN1	NF1	DRASTIC
Model-2	NN2	NF2	DRASTIC DH
Model-3	NN3	NF3	DRASTIC,DH,PED
Model-4	NN4	NF4	DRASTIC,DH,PED LULC
Model-5	NN5	NF5	DRSI
Model-6	NN6	NF6	DRSI DH
Model-7	NN7	NF7	DRSI DH PED
Model-8	NN8	NF8	DRSI DH PED LULC
Model-9	NN9	NF9	DH PED LULC
Model-10	NN10	NF10	PED_DH_BD
Model-11	NN11	NF11	PED_DH_BD_LULC
Model-12	NN12	NF12	pH_OM_BD
Model-13	NN13	NF13	DRASTIC, LULC
Model-14	NN14	NF14	DRSI, LULC

3.6 Coincidence reports

Once the vulnerability maps were generated using the above methods, field data were used to generate coincidence reports to evaluate their performances. Water quality data for E Coli for 55 wells were used in this study. The well water quality data we provided by FL Dept. of Environmental Protection (FLDEP). Sixteen out of 55 wells were contaminated with at least one occurrence ce of E Coli. It was assumes 1 E coli is an indicator of the presence of contamination movement pathways. A set of coincidence reports was generated between vulnerability maps and well contamination data to compare actual contamination with potential contamination (or vulnerability) generated by our models.

4. RESULTS AND DISCUSSION

4.1 Training of NN model

The Table 7 shows training results of the NN. Internally each category in the classification output is considered to be mutually exclusive and is assigned an output node in the neural net. The relative entropy measure ensures that the outputs of the NN enforce the mutual dependence of the outputs. It maximizes the probability of successful classification. Ideally a very low value of relative entropy

indicates a good fit of the model to the data. The accuracy gives the fraction of records whose prediction is within a specified tolerance of the desired output. By default the accuracy tolerance is set to 20% of the range of the output.

Table 7. NN Models: Performance of Training Data.

Model name	Patterns	Training Set Accuracy	Test Set Accuracy	All Data Accuracy	Relative Entropy		
					Train	Test	All
DRASTIC DH	1733	0.86314	0.857692	0.861512	0.09899	0.108067	0.101714
DRASTIC DH PED	2675	0.873397	0.902864	0.882243	0.115352	0.125596	0.118427
DRASTIC DH PED LULC	7159	0.787867	0.799348	0.791312	0.143857	0.151916	0.146275
DRSI	55	1	0.945455	0.945455	0.003272	0.032348	0.032348
DRSI DH	502	0.766382	0.774834	0.768924	0.16442	0.16174	0.163614
DRSI DH PED	830	0.817241	0.8	0.812048	0.191069	0.188303	0.190236
DRSI DH PED LULC	NA	NA	NA	NA	NA	NA	NA
DH PED LULC	160	0.873874	0.857143	0.86875	0.08823	0.121458	0.098406
PED_DH_BD	57	1	0.929825	0.929825	0.006575	0.016977	0.016977
PED_DH_BD_LULC	256	0.73743	0.688312	0.722656	0.206299	0.203072	0.205329
pH_OM_BD	NA	NA	NA	NA	NA	NA	NA
DRASTIC, LULC	NA	NA	NA	NA	NA	NA	NA
DRSI, LULC	187	0.938462	0.929825	0.935829	0.078415	0.077921	0.078264

4.2 Training Results of NF model

The Table 8 shows characteristics of training data used with the Neuro-fuzzy models. For the model NF1, the variable R showed maximum SD whereas for the models NF2 and NF3 variable D showed the maximum SD.

Table 8. Characteristics of Training Data for Neuro-fuzzy Models.

Variable	Name	mean	SD	minimum	Maximum	Missing
		NF 1				
Var 1	D	8.07	1.93	3	10	0
Var 2	R	3.6	2.79	1	10	0
Var 3	S	3.77	2.44	0	9	0
Var 4	I	7.09	1.82	3	10	0
		NF 2 and NF 3				
Var 1	D	16.92	14.90	3	63	0
Var 2	R	3.6	2.79	1	10	0

Var 3	S	3.77	2.44	0	9	0
Var 4	I	20.03	13.44	10	63	0

Table 9 shows performance of the training data used with Neruo-fuzzy models. NF2 showed highest number of misclassification as well as error. This error corresponds to the sum of squared differences between targets and outputs and is a measure of the ambiguity of classifications.

Table 9. Neuro-fuzzy Models: Performance of Training Data.

Name of Model	Patterns	Accuracy (%)	Misclassifications(%)	Error
DRASTIC DH	1733	62.84	37.16	1170.98
DRASTIC,DH,PED	2677	75.57	24.43	1233.6
DRASTIC,DH,PED LULC	7159	84.73	15.27	2397.67
DRSI	55	80	20	25
DRSI DH	502	58.96	41.04	394
DRSI DH PED	832	79.81	20.19	363.6
DRSI DH PED LULC	NA	NA	NA	NA
DH PED LULC	160	82.5	17.5	66.7
PED_DH_BD	57	71.93	28.07	24.45
PED_DH_BD_LULC	256	80	20	85
pH_OM_BD	NA	NA	NA	NA
DRASTIC, LULC	NA	NA	NA	NA
DRSI, LULC	183	90.16	9.84	41.1

4.3 Sensitivity Analysis of NN and NF

4.3.1 Vulnerability maps

The models described below were created in a GIS by incorporating the various permutation combination of 14 parameters D, R, A, S, T, I, C, BD, DH, LULC, Soils structure and pedality. The same training data sets were used for models are shown in (Tables 6 and 7). Spatial distribution of vulnerability category varied from models to models (Figures 3 and 4). Due to sheer number of we are going to summarize the most interesting simulations in the main document. Please find the comprehensive simulation results in the Appendix B. Table 10 shows summery of areal coverage for the selected models.
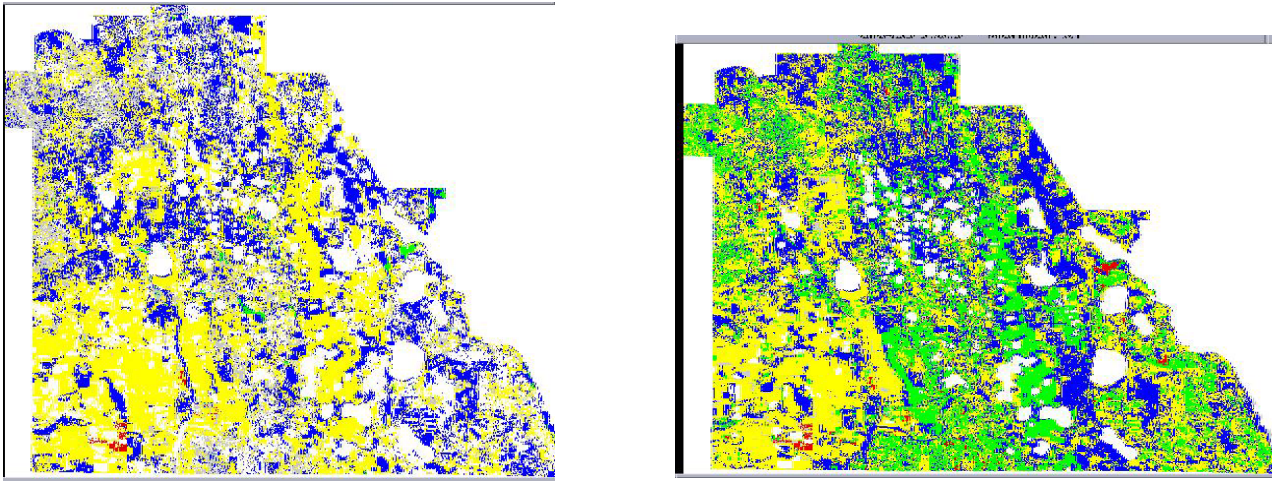
Figure 3. Spatial Distribution of vulnerability categories from the model using DH, ped, LULC parameters using NF (left); using NN(right)
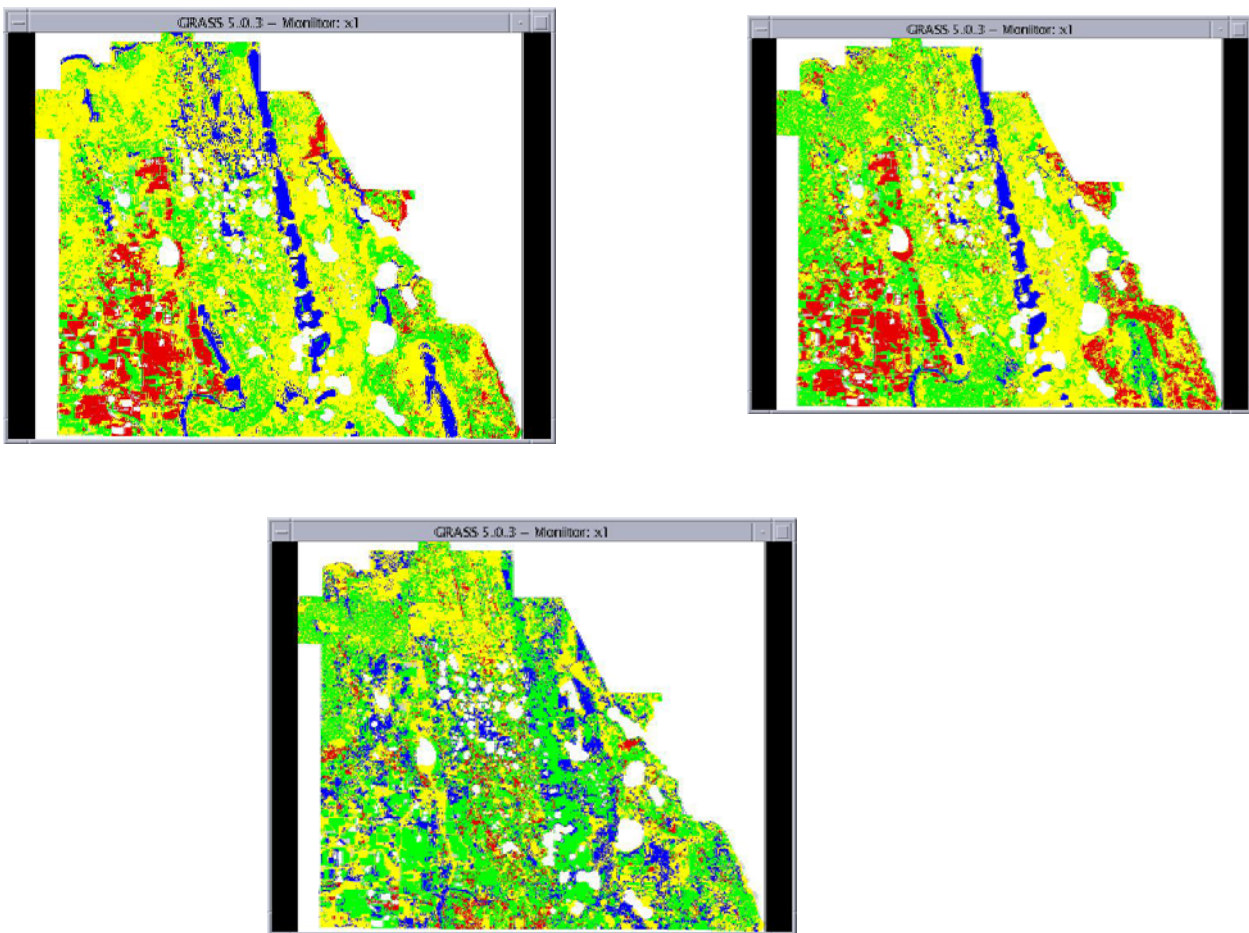
Figure 4. Spatial Distribution of Vulnerability from Neural networks models: (left NN2, right NN3, and bottom NN4). **Parameters and model names***: Drastic DH (NN2), DRASTIC DH, Ped (NN3), DRSTIC , DH, Ped, LULC (NN4)*
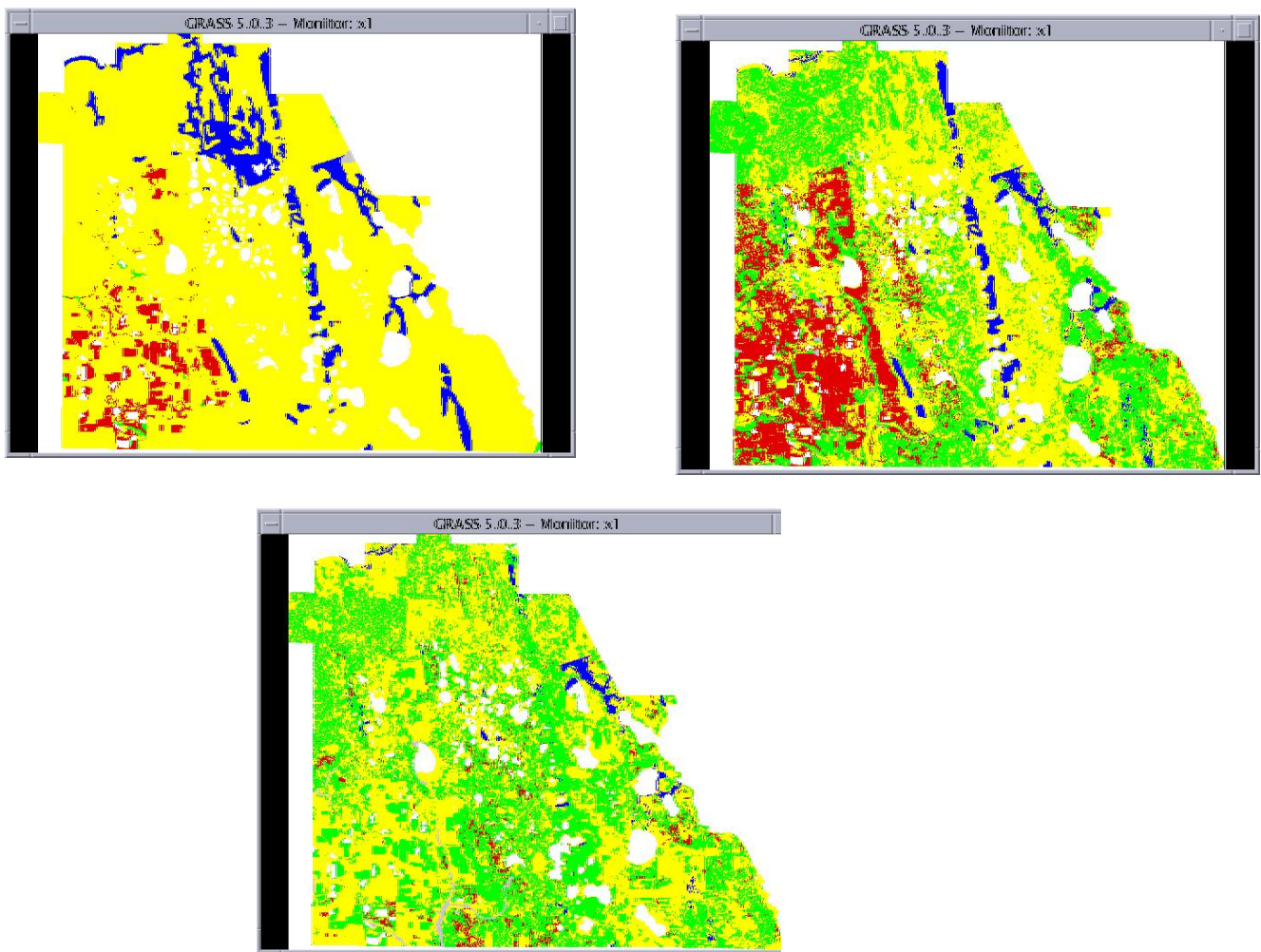
Figure 5. Spatial Distribution of Vulnerability from Neuro-fuzzy models: (left NF2, right NF3, and bottom NF4).). **Parameters and model names***: Drastic DH (NN2), DRASTIC DH, Ped (NN3), DRSTIC , DH, Ped, LULC (NN4)*

Table 10. Spatial Distribution of Vulnerability Categories in Percentage: Selected Models.

Vulnerability Categories	Area Coverage by the Models (%)					
	NN2	NF2	NN3	NF 3	NN4	NF4
Not classified/no data	2	0	2	0	2	1
Low	9	8	5	3	16	2
Moderate low	54	87	47	51	36	54
Moderate	24	0	30	29	42	41
High	11	5	15	16	5	2
Total	100	100	100	100	100	100

4.3.2 Coincidence Reports

Coincidence reports between vulnerability maps and well data were generated using GRASS raster files (Figures 6- 9). A total of 28 models were created using neural networks and neuro-fuzzy methods ((14 each). All models were compared to DRASTIC model too. NN2 performed reasonably good in predicting contaminated wells – it did not perform well while classifying non-contaminated wells. NN2 predicted 5 out of 7 contaminated wells as highly vulnerable category whereas 25 of the non-contaminated wells were classified as in the high category. A well performing NN or NF model should be able to classify contaminated wells in high category and non-contaminated wells in low or moderately low vulnerability category. The model NN5 (DRSI) predicted 8 contaminated wells as highly vulnerable and 1 well each in the low and moderately low vulnerability category, respectively. NN7 (DRSI,DH,ped) and model NN11 predicted equal number of contaminated wells in the highly vulnerable category. However, all these 3 models (NN5, NN7 and NN11) over predicted non-contaminated wells. The comparison of point data to a spatial data for accuracy assessment is not the ideal way. The coincidence analysis was performed to get an idea of how the models are performing in a relative sense. These values should not be used as absolute indicators of the suitability of models. Although the coincidence reports show similar trend for NF 7 and NN7, NF 5 showed drastically different results than NN5. In general, NF models showed higher uncertainty than the NN models while predicting contaminated wells.
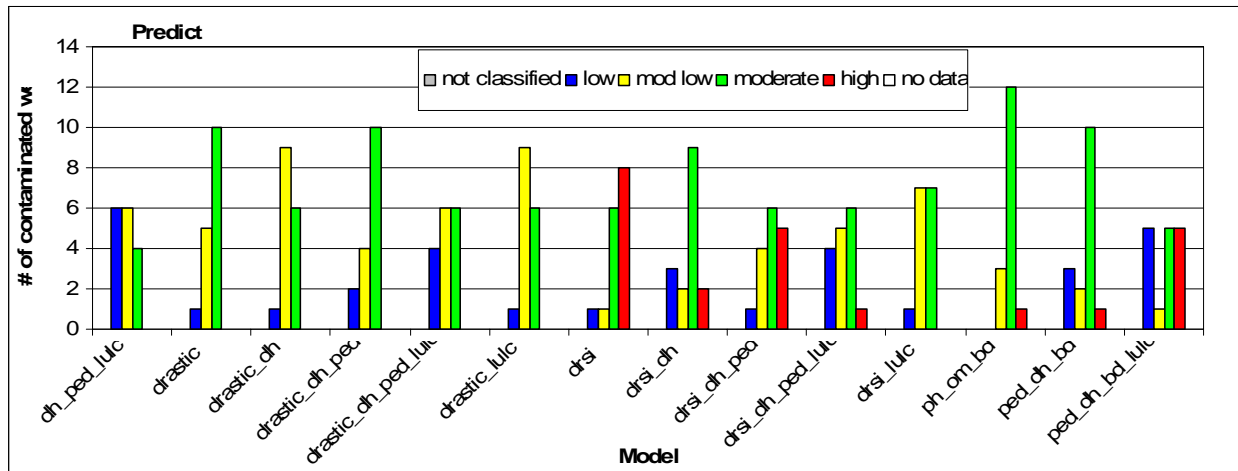
Figure 6. Coincidence report for NN models and well water quality data E Coli data
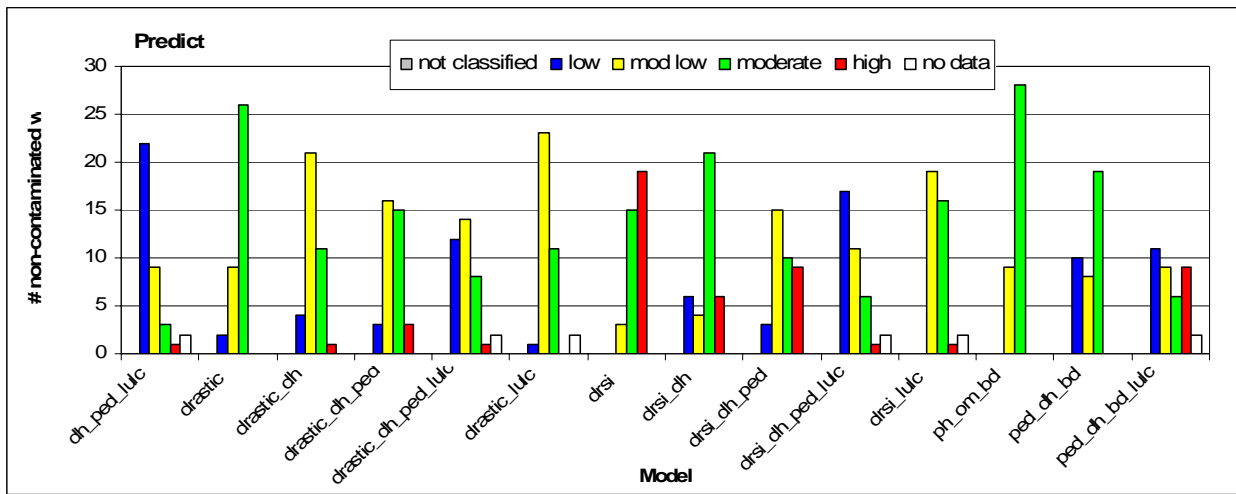
Figure 7. Coincidence report for NN models and non contaminated wells
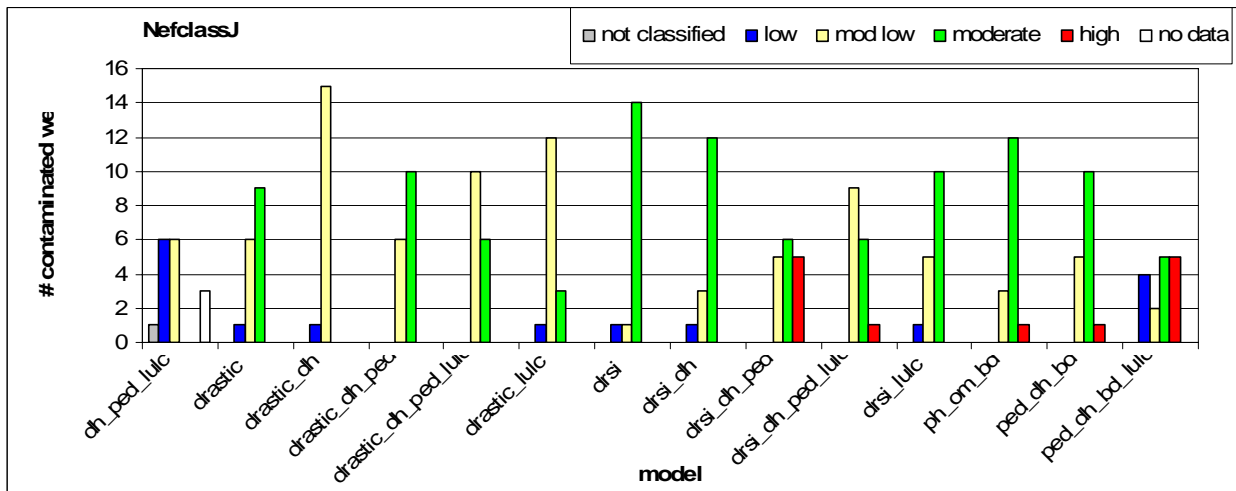
Figure 8. Coincidence between neuro-fuzzy models and contaminated wells (E Coli).
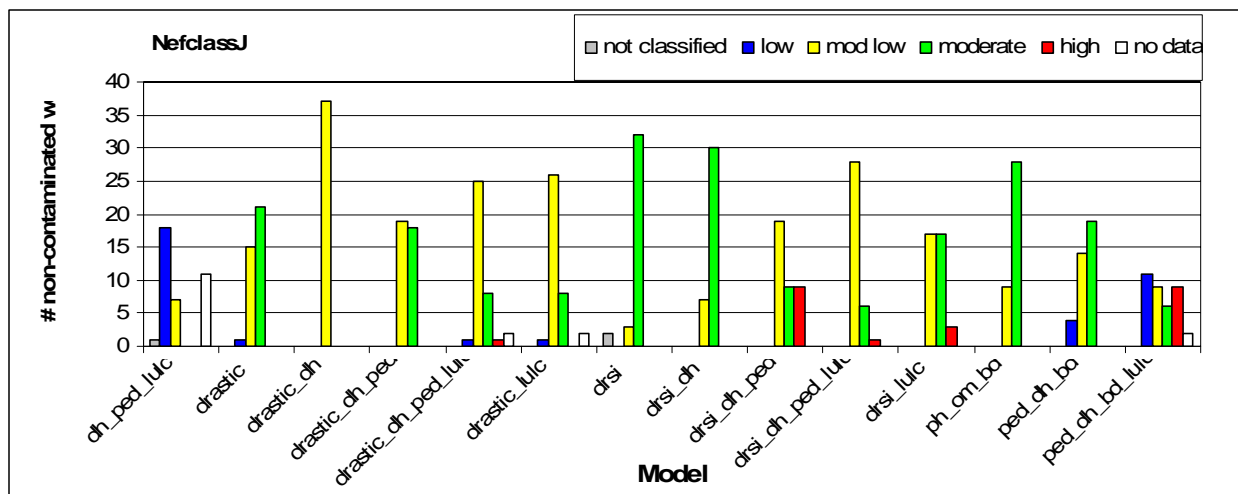
Figure 9. Coincidence report between neuro-fuzzy models and non contaminated wells.

5. CONCLUSION

Compared to Neuro-fuzzy models, NN models performed better with contradictory data. Coincidence reports with well water quality data did not yield conclusive results, nor should they be used as absolute indicators. Although for our project integration and use of NN software with GIS was cumbersome and time consuming – it predicted better. With the fine-tune of the contradictory data manually could yield similar vulnerability maps both from NN and Neuro-fuzzy models and improve well predictions. Further studies needed. A larger data set of well contamination may provide better results.

References

1. Aller, L. T., J.H. Bennett, R. Lehr, J. Petty, and G. Hackett. 1987. DRASTIC: A Standardized System for Evaluating Ground Water Pollution Potential Using Geo-Hydrogeologic Settings. U.S. Environmental Protection Agency Report. EPA600/2-87/036.
2. Burrough, P.A., R.A. MacMillan, and W. Deursen. 1992. Fuzzy classification methods for determining land suitability from soil profile observations. J. Soil Sci. 43:193-210.
3. Burrough, P. A. 1996. Opportunities and Limitations of GIS-based Modeling of Solute Transport at the Regional Scale. In *Application of GIS to the non-point source pollutants in the vadose zone*, SSSA, Special Publication # 48, D. Corning and K. Loague eds., Madison, WI.
4. Corwin, D. L, K. Loague and T. R. Ellsworth. 1996. Introduction to Non-Point Source Pollution in the Vadose Zone with Advanced Information Technologies. In: Assessment of Non-Point Source Pollution in the Vadose Zone, ed. D. L. Corwin, K. Loague and T. R. Eliisworth. Geophysical Monograph 108. AGS, Washington D.C
5. Dixon, B. "Application of neuro-fuzzy techniques to predict ground water vulnerability in NW Arkansas." Ph.D. diss., University of Arkansas, 2001.

6.Dixon, B., H.D. Scott, J.C. Dixon, and K.F. Steele. 2002. Prediction of Aquifer Vulnerability to Pesticides Using Fuzzy Rule-Based Models at the Regional Scale. Physical Geography 23:130 – 152.

7.De Gruijter, J. J, D. J. J. Walvoort, and P. F. M. Van Gaans. 1997.   Continuos soil maps - a fuzzy set approach to bridge the gap   between aggregation levels of process and distribution models. Geoderma. 77:169-195.

8. Khan, E. 1999. Neural fuzzy based intelligent systems and applications. In *Fusion of neural networks, fuzzy sets, and genetic algorithms: Industrial applications*, edited by L.C. Jain and N.M. Martin. CRC Press, Washington, D.C. p. 331.

9. Nauck, U. and R. Kruse. 1999. Design and Implementation of a neuro-fuzzy data analysis tool in JAVA. Manual. Technical University of Braunschweig. Germany.

10. Smith, P. A., Scott, H.D., and Fugitt, T. (1994). Influence of geographic database scale on prediction of groundwater vulnerability to pesticides. *Journal of Soil Contamination*, Vol. 3, 285-298.

11. Wang, F., G. Hall and Subaryono. 1990. Fuzzy information representation and processing in conventional GIS software: database design and application, Int. J. GIS. 4:261-283.

Mechanisms and Modeling of Soft-Bed Nutrient Release in Lakes

Basic Information

Title:	Mechanisms and Modeling of Soft-Bed Nutrient Release in Lakes
Project Number:	2005FL101B
Start Date:	3/1/2005
End Date:	2/28/2006
Funding Source:	104B
Congressional District:	10th
Research Category:	Ground-water Flow and Transport
Focus Category:	Non Point Pollution, Nutrients, Sediments
Descriptors:	None
Principal Investigators:	Ashish J Mehta

Publication

1. Jain, M., Mehta, A. J., Hayter, E. J., and Di, J., 2006. Fine sediment resuspension and nutrient transport in Newnans Lake, Florida, submitted for publication in the proceedings of INTERCOH 2005 meeting, T. Kusuda, H. Yamanishi and E. Toorman eds., Elsevier, Amsterdam.

Fine Sediment Resuspension and Nutrient Transport in Newnans Lake, Florida

Mamta Jain[1], Ashish J. Mehta[1], Earl J. Hayter[2] and Jian Di[3]

[1] Department of Civil and Coastal Engineering
University of Florida, Gainesville, FL 32611, U.S.A.

[2] U.S. Environmental Protection Agency
Athens, GA 30605, U.S.A.

[3] Environmental Sciences Division
St. Johns River Water Management District
Palatka, FL 32178, U.S.A.

Abstract

The character of fine sediment resuspension and nutrient transport were examined for Newnans Lake in north-central Florida. Physical and water quality parameters were monitored over a period of eight months in the lake and also in the inflow and outflow streams. From the hydraulic point of view, this lake may be thought of as a shallow and wide open channel in which inflowing sediment transport is modulated by wind effects. Suspended sediment concentration (SSC) response to wind speed was found to occur over a wide frequency band, with spectral peaks that seemingly correlate with lunar motion. On a time-mean basis, wind kinetic energy maintains the particulate matter as a Benthic Suspended Sediment Layer with a mean height of about 0.80 m and SSC of about 70 mg L^{-1}. The suspended sediment mass per unit bed area is equivalent to less than 1 mm thick bed layer, indicating that there is little interaction between the ~ 2 m thick muck in the lake and the water column. Nutrient mass balance analysis is simplified because dissolved nutrient loads are close or nearly equal to total loads, with minor to negligible contributions from the low-concentration particulate matter. Mass balances for

phosphorus and nitrogen indicate periods of days over which the lake acts both as a net exporter and a net importer of these nutrients.

INTRODUCTION

In recent decades several lakes in Florida have attained high trophic levels and their water quality has become a matter of concern to the management agencies. Such lakes tend to be laden with fine-grained, organic-rich muck at the bottom, which can be a repository as well as a source of phosphorus and nitrogen necessary for the eutrophication. Since these nutrients are typically derived from inflow streams, an important question bearing on water quality management is the role of these streams and sediment resuspension in the lake in governing nutrient loads in the outflow streams. In lakes where water throughput is steady and sufficiently high to ensure low residence times for water parcels and suspended matter, an assessment of water quality does not always require a lengthy diagnostic treatment. On the other hand, where throughput is high only on an episodic basis, the transport process can be complex because under normal conditions effects due to stream discharge and wind tend to occur at uncorrelated frequencies. Given that most lakes in Florida experience episodic forcing, as a paradigm we examined Newnans Lake in north-central Florida, with the aim to assess its sediment and nutrient transport regimes. A factor as well in the selection of this lake was the State of Florida's plan to restore the lake's water quality in the coming years.

Although water quality and biological assays have been carried out in the lake, prior information on sediment and nutrient transport in the combined lake-and-stream system is sparse. Therefore, in 2004 we conducted a field campaign to obtain time-series and discrete sampling measurements related to factors characterizing the transport regime.

Data included stream discharges, wind-induced hydrodynamic parameters, suspended solids concentration (SSC) and concentrations of chemical species related to the nutrients (phosphorus and nitrogen). Observations based on these data are summarized, and an effort has been made to characterize the sediment and nutrient transport regimes.

SITE AND METHOD OF ANALYSIS

The 7 km long and 4 km wide lake in north-central Florida (Fig. 1) has a surface area of about 27 km^2. The lake has up to 2 meters of muck, and portions of the littoral zone are densely covered by floating macrophytes that have contributed to the organic component of the muck. The maximum depth of water is about 3.9 m in the middle of the lake and the mean depth about 1.6 m. Thus the volume of muck, about $2x10^7$ m^3, constitutes over one-half the lake volume above the sandy substrate beneath the muck. The muck is watery with a mean dry density of about 100 kg m^{-3}, which corresponds to a solid mass of two million metric tons. At the present rate of sediment inflow, this amount would be equivalent to over eight centuries of sediment from the drainage basin.

The lake drainage area covers approximately 300 km^2 and supplies the majority of the runoff through two main tributaries, Hatchet Creek and Little Hatchet Creek, both at the northern end of the lake. A smaller stream called Bee Tree Creek confluences with Hatchet Creek north of its outlet at the lake. Overflow drains out of Prairie Creek at the southern end and empties into a large basin called Paynes Prairie. The majority of the lake shoreline is surrounded by a canopy of local forest trees.

At the site shown in Fig. 1, a three-legged aluminum-frame platform schematically drawn in Fig. 2 was installed in December 2003, and fully operated from early January to early September in 2004. Transducers (Table 1) were deployed for measuring wind

3

velocity, air and water temperatures, total water pressure and pore water pressure within muck, horizontal and vertical current velocity components, wave-induced acceleration in muck, SSC in water (at three levels) and water samples (two levels).

Data on current velocity, total water pressure, pore water pressure, and fluid (muck) acceleration were collected in the digital mode. Sampling was on the hour for 5 minutes at a bursting frequency of 10 Hz. Wind speed, air temperature, water temperature, air pressure and SSC data collection was in the analog mode with 2-min mean values recorded every one-half hour. All data were telemetered on real-time basis via a modem and cell-phone connection to the University of Florida for storage and analysis.

At stations BTC, HC, LHC and PC, daily discharges were measured by the St. Johns River Water Management District (SJRWMD). Also measured at these stations and at HCW were water quality parameters. At NL daily lake water level data were recorded, and at GNV (Gainesville Regional Airport) daily values of atmospheric parameters were recorded by the airport authority (Jain et al., 2005). A description of the bottom sediment characteristics has been presented by Gowland et al. (2005). For the 0.4 m thick top layer of bottom sediment relevant to the present study the ranges of bed parameters were as follows: Stokes' settling diameter of aggregated particles 26 to 38 μm, organic matter 43 to 52% by weight, wet bulk density 1,020 to 1,050 kg m^{-3}, and particle density 1,600 to 2,100 kg m^{-3}.

The vertical profile of the bed bulk density obtained by a 76 mm diameter PVC push-core is shown in Fig. 3. As indicated, the accelerometer and the pore pressure gauge were both located 0.2 m below the muck surface. This was arranged in order to determine if the muck heaved due to wind wave action. At that depth the (wet bulk) density was

4

approximately 1,046 kg m^{-3}, which indicated that the muck had negligible (bulk) shear strength (Mehta, 1991).

The erodibility characteristics of the bottom muck were determined in laboratory tests reported by Gowland et al. (2005). Bed erosion was modeled by the equation

$$\varepsilon_e = \varepsilon_N (\tau_{cw} - \tau_s) \tag{1}$$

where ε_e is the erosion flux, ε_N is the erosion flux constant, τ_{cw} is the peak value (over the wave period) of the combined bed shear stress due to current and waves, and τ_s is the bed shear strength against erosion. For modeling sediment transport, a lake-mean value of ε_N = 1.0 kg m^{-2} s^{-1} Pa^{-1} was selected, and τ_s was determined by calibration against measured SSC time-series. We used the following functions to describe the settling flux ε_s:

$$\varepsilon_s = w_o C, \quad C < C_o; \qquad \varepsilon_s = \frac{a\,C^n}{\left(b^2 + C^2\right)^m}, \quad C \geq C_o \tag{2}$$

in which C denotes SSC and C_o (= 0.1 kg m^{-3}) is the concentration limit below which w_s tends to be practically free of the effect of inter-particle collisions and is assumed constant (w_0 = 1.15x10^{-4} m s^{-1}). The coefficients $a, b, n,$ and m were taken as 0.17, 2.4, 1.8 and 1.8, respectively.

The shear stress τ_{cw} was determined from the method of Soulsby et al. (1993). To being with, the current-induced shear stress τ_c was determined from

$$\tau_c = \left[\frac{0.4}{\ln(0.033h/k_s) - 1} \right]^2 \rho_w u_m^2 \tag{3}$$

where h is the water depth, k_s is the Nikuradse bed roughness, ρ_w is the fluid (water) density and u_m is the near-bottom current velocity. The wave-induced bed shear stress was calculated from

$$\tau_w = 0.5 f_w \rho_w \left(\frac{H\sigma}{2\sinh kh} \right)^2 \tag{4}$$

where f_w is the wave friction factor, H is the wave height, $\sigma = 2\pi / T$ is the wave angular frequency, $k = 2\pi / L$ is the wave number, T is the wave period and L is the wavelength. The wave friction factor was obtained from

$$f_w = 0.3, \quad \frac{a_b}{k_s} \le 1.57; \quad f_w = 0.00251 \exp\left[5.21 \left(\frac{a_b}{k_s} \right)^{-0.19} \right]; \quad \frac{a_b}{k_s} > 1.57 \tag{5a}$$

where the wave-induced bottom excursion amplitude a_b is given by the Airy linear wave theory (Dean and Dalrymple, 1991) as

$$a_b = \frac{H}{2\sinh kh} \tag{5b}$$

The current and wave shear stresses are superimposed using

$$\begin{aligned} Y &= 1 + a_o X^M (1-X)^N \\ Y &= \frac{\tau_{cw}}{\tau_c + \tau_w} \\ X &= \frac{\tau_c}{\tau_c + \tau_w} \end{aligned} \tag{6a}$$

where

$$a_o = \left(a_1 + a_2 |\cos\varphi|^I \right) + \left(a_3 + a_4 |\cos\varphi|^I \right) \log \left\{ \frac{f_w}{\left[0.4 / \{\ln(0.033 h / k_s) - 1\} \right]^2} \right\} \tag{6b}$$

with analogous expressions for M and N. The quantity φ is the angle between the current stress vector and the wave stress vector. The coefficients a_i, M_i, N_i (i = 1 to 4) and I are given in Table 2, as prescribed by Soulsby et al. (1993).

The above formulation for calculating τ_{cw} requires values of h, H, T, L, u_m, φ and k_s. For the water depth h a recent bathymetric survey was used (Jain et al., 2005). The wave

length L is dependent on height H and period T, and the Airy theory was used to relate the three, with H and T obtained from measurements.

For determining u_m and k_s we used the public domain numerical model Environmental Fluid Dynamics Code (EFDC), a three-dimensional, hydrostatic flow model with a compatible sub-model for sediment transport. The Cartesian coordinate system was used in the horizontal plane, and the vertical coordinate was stretched to follow the bottom contours and the free surface. In the model the finite difference method is used to solve the governing equations, and an external/internal mode splitting procedure is used to increase numerical efficiency (Hamrick, 1992; 1996; 2000; Park et al., 2001). As the model generated the instantaneous current velocity vectors throughout the lake and the wind direction was known in principle, the angle φ could have been determined. However, for simplicity of treatment, φ was set equal zero everywhere.

The sediment sub-model of EFDC solves the mass balance equation for SSC. Due to a small numerical diffusion inherent in the scheme used to solve this equation, the horizontal diffusion terms are omitted. Equations (1) and (2) were used to calculate the erosion and deposition fluxes required as the important bottom boundary conditions for the sub-model.

OBSERVATIONS

Monthly values of the physical parameters listed in Tables 3 and 4 characterize the lake as one subject to moderate climatic changes. The directionally variable winds (Fig. 4) are low-energy; the mean wind speed rarely exceeds 10 m s^{-1}. High speeds in June-September were due to the passage of Hurricanes Frances and Jeanne over northern

Florida in September. Current speed measured at the platform was on the order of only a few millimeters per second (Table 5).

Although the monthly maximum value of the significant wave height (derived from water pressure data) was 0.28 m in June, typical values ranged between 0.14 and 0.16 m. The maximum value of the modal period was 1.4 s. Besides low wind speeds, wave action in the lake is limited by shallow water depths and short wind fetches. The maximum fetch at the platform was less than 4 km.

It proved to be difficult to determine the precise depth of the muck surface at the platform because SSC changed gradually with depth, so the bed was not defined by a distinct interface. The effective water depth was therefore estimated by comparing the measured amplitudes of wave orbital current and vertical acceleration (Table 4) with the same quantities calculated from the Airy theory in which the water depth was adjusted until a match occurred. This led to a value of depth $h = 2.1$ m.

In Table 3, discharge out of Prairie Creek does not correlate with rainfall because of the significant effect of evapotranspiration on the lake's water budget, especially during the summer months (May-August). In contrast, contribution from groundwater or seepage is believed to be minor. Due to shallow water, significant thermoclines typically do not develop even as pycnoclines due to SSC and nutrients persist. Vertical gradients in SSC are evident from the values given in Table 5.

The main tributary to the lake is Hatchet Creek, as Little Hatchet Creek contributes, on the average, only about 20% of the total inflow. However, under normal conditions neither discharge from Hatchet Creek nor wind is dominant as a transporting agent in the lake proper. As a result, the combined influence of discharge and wind on SSC is

manifested as a noisy signal spread over a wide frequency band. This is evident in Fig. 5, in which a sample of the measured SSC time-series (by OBS-2) suggests multi-frequency response. The running average curve represents frontal oscillations on the order of days, and these fluctuations are modulated by higher frequency diurnal contributions.

Figure 6 shows wind, air temperature and SSC spectra derived from a 90-day long (January-March) time-series. Three noteworthy peaks are seen, and they seem to be related to lunar tidal harmonics. These are the lunar quarter-phase period of 6.8 solar days, its second harmonic of 3.4 d and the lunar diurnal period of 1.08 d. A fourth peak corresponding to about 0.5 d could be the luni-solar semi-diurnal period (11.97 hr). Sea breeze is known to respond to tidal effects (Richards, 2003), and is the seeming explanation for the coincidence of the frequencies with lunar motion. Nonetheless, the occurrence of this effect is somewhat surprising because the lake is approximately 100 km from the Atlantic coast, a substantial distance. A further study of meteorological forcing is essential before a definitive conclusion can be reached as to the interpretation of the observed spectral peaks.

From Tables 3 and 4 we observe that monthly mean wind speeds range between 2.5 and 4.1 m s^{-1}, and monthly peak winds between 8.9 and 12.6 m s^{-1}. The generally low mean and peak speeds point to a practically "eventless" period of eight months. Similarly, the Prairie Creek discharge range of 0.21 to 1.24 m^3 s^{-1} indicates consistently low throughput over the same period. Higher wind speeds in September accompanying the hurricanes also brought higher rainfall and creek discharges. On September 9, following the nearest passage of Frances on September 4, discharge in Prairie Creek rose to 22 m^3 s^{-1}. Then, on September 30, following Jeanne on September 25, the discharge

further increased to 27 m^3 s^{-1}. 2-min mean gusts attained maximum values of 20 m s^{-1} during Frances and 15 m s^{-1} during Jeanne. It should be pointed out, however, that in the recent past hurricanes have seldom led to high discharges coupled with high winds in this region of Florida. More common occurrences are those of high discharge without high wind, as during the El Niño event of February 1998 when the peak discharge in Prairie Creek was 17 m^3 s^{-1}.

Wave related parameters showed a weak but identifiable dependence on wind speed. A typical set of data is from the month of February. In Fig. 7 the significant wave height is seen to increase with wind speed at a nearly linear rate. The cutoff line at 2 m s^{-1} corresponds to the limit of sensitivity of the wave pressure gage. In Fig. 8 the wave modal period is also seen to increase with wind speed, albeit in a non-linear way. In Fig. 9, plots of the horizontal and vertical wave velocity amplitudes are given. These amplitudes are consistent with the wave height (Fig. 7) and period (Fig. 8) data.

To help interpret the relationship between SSC (C) and wind speed (U), each was represented by the sum of a low-frequency component (marked by an overbar) associated with frontal wind events and a higher frequency component (with a hat) associated with daily (diurnal) events:

$$U = \bar{U} + \hat{U} ; \qquad C = \bar{C} + \hat{C} \tag{7}$$

In Figs. 10a,b data from OBS-2 have been plotted. The $\bar{C}$ values show a weak yet recognizable linear dependence on $\bar{U}$ ($\bar{C} = \bar{a}\bar{U} + \bar{b}$). In Fig. 10b, $\hat{C}$ shows little dependence on $\hat{U}$. Nevertheless, for the convenience of data interpretation, one may postulate the occurrence of a linear relationship of the form $\hat{C} = \hat{a}\hat{U}$. Values included correspond to times when $\hat{U}$ and $\hat{C}$ were increasing together, i.e., when both quantities

had positive slopes. Data at times when either (or both) slope of a $\hat{U}, \hat{C}$ pair was negative had to be discarded in order to avoid even more excessive data scatter than observed. A likely reason for this lack of response of $\hat{C}$ to $\hat{U}$ may be that the ratio of the wave period (~ 1 s) to the sediment settling time lag (~10^{-4} m s^{-1}) was on the order of 10^{-4}, a very small value. As a result, and coupled with a directionally variable wind-wave field which complicated the role of waves, discrete oscillations in SSC induced by settling and entrainment could not be clearly gleaned from the data.

Taking $\bar{U}$ = 4 m s^{-1} and $\hat{U}$ = 0.5 m s^{-1} as representative values we obtain $\hat{C}/\bar{C}$ = 0.4/16.5 = 0.02. In Table 6 this ratio is calculated for the three OBSs. Also given are the coefficients $\bar{a}, \bar{b}$ and $\hat{a}$. To enhance the generality of the observations, results are included from February (representing the winter climate) as well as May (representing summer), when unfortunately only two of the three sensors were operating. Overall, the $\hat{C}/\bar{C}$ ratio ranges from 0.02 to 0.11, indicating that diurnal variations modulate the frontal amplitudes by a factor of 2% to 11%. In other words, daily winds seem to play a lesser role compared to "weekly" wind events in resuspending sediment.

In Fig. 11, the suspended sediment load S is plotted against discharge Q for Prairie Creek. The mean trend is seen to be linear, which implies a constant SSC (C = 16 mg L^{-1}), because by definition $S = CQ$. These data are based on samples collected at mid-depth in the creek, and in terms of elevation they are compatible with data recorded by OBS-2 in the lake. Data from Hatchet and Little Hatchet Creek also indicated similar trends, with mean concentrations given below.

Hatchet (+ Bee Tree) Creek	8 mg L^{-1}
Little Hatchet Creek	11 mg L^{-1}
Prairie Creek	16 mg L^{-1}

Constant SSC in the creeks implies that sediment transport in these streams is supply-limited. The inflow creek beds appear to consist of sediment that does not erode even at high discharges, a characteristic of channels in clear-water equilibrium. In Prairie Creek, SSC is limited by supply from the lake.

FLOW FIELD AND SEDIMENT TRANSPORT

For simulation of the flow field and sediment transport using the EFDC model, the Cartesian grid for the lake was composed of 1078 computational cells. The horizontal dimension of each cell was 150 m (N-S) by 100 m (E-W). Three stretched horizontal layers were used to represent the water column. At the lake boundary cells representing the three creeks, measured discharge time-series were supplied. Also inputted into the model were time-series of wind, precipitation and evapotranspiration. The wave height and period fields required for bed shear stress calculation were estimated from relationships with wind speed of the type shown in Figs. 7 and 8, respectively. At the cell containing the water level gauge (NL in Fig. 1), the measured time-series was compared with simulation. The hot-start calibration period was from day 5 to 54, and the best agreement was obtained using a bed roughness parameter $k_s = 0.01$ m. Validation covered the period from day 60 to 110.

A comparison between measured and simulated water levels in the lake in Fig. 12 during validation shows a reasonable agreement, with a maximum difference of about 0.08 m before day 99 and about -0.02 m afterwards. During the 50-day period the simulated water volume out of Prairie Creek was 7.62×10^6 m^3, which differed from the measured value (7.73×10^6 m^3) by less than 2%.

Figure 13 shows the simulated surface velocity vectors in the lake for a selected southwesterly wind of 7 m s^{-1} and a steady outflow of 1.3 m^3 s^{-1} out of Prairie Creek in February 2004. Due to the throughput from the inflow creeks towards Prairie Creek, the vectors point southward, with the exception of littoral circulation gyres generated by local boundary geometry. The velocities were everywhere below 0.03 m s^{-1}. It is also noteworthy that in the southern part of the lake the flow is channelized through a seemingly narrow neck. A similar simulation without wind produced lower velocities, which fell by about 40% in the neck area.

The fine sediment transport sub-model in EFDC was calibrated by adjusting the erosion shear strength τ_s (= 0.035 Pa) to achieve agreement between measured and simulated time-mean SSC values at the platform. Figure 14 shows the comparison over a 10-day period in February for OBS-1 and OBS-3. The OBS-2 data were intermediate between these two and are not plotted. While a reasonable agreement for the 10-day mean values is achieved (Table 7), measured SSC is seen to be substantially less time-dependent than the simulated values. For example, whereas at OBS-3 the measured mean amplitude of this variation (about the time-mean value) is about 50 mg L^{-1}, the corresponding value for the simulated SSC is about 5 mg L^{-1} in agreement with Fig. 10a. As described next, this order of magnitude difference between simulated and measured amplitudes of SSC requires invocation of a hydraulic open channel analogy of the lake-and-streams system.

LAKE REGIME

Newnans Lake can be viewed as the wide segment of a narrow water course or channel. The up-lake reach of the channel is a notional water course combining Hatchet

Creek and Little Hatchet Creek. Prairie Creek is the down-lake reach of the same channel. Within the lake the speed of the channel current is reduced substantially, while at the same time wind generates waves and a very weak circulation. The combined strength of the current and circulation is only a few millimeters per second.

Suspended sediment is present in the lake at all times, with a representative SSC profile shown in Fig. 15. The SSC gradient, called a secondary lutocline (Ross and Mehta, 1989), defines what may be referred to as a Benthic Suspended Sediment Layer (BSSL) beneath the gradient. The lower level of this weakly non-Newtonian layer is the primary lutocline characterized by hindered settling below this lower lutocline. For the present analysis we may conveniently chose the muck-water surface to represent the lower bound of the BSSL. The BSSL shown does not have a well defined height but it can be taken as 0.80 m based on the "equal area" assumption, which idealizes the water column as composed of a distinct BSSL beneath sediment-free water. This value is a representative mean for the entire period of measurement, with a range of about 0.2 to 1 m.

The thickness of the bottom sediment layer that must be entrained to generate the 0.80 m high BSSL with a mean SSC of about 70 mg L^{-1} (Fig. 15) can be estimated. Taking 100 kg m^{-3} as the dry density of the bed, this thickness is equal to (0.07/100)x0.80 = 0.00056 m = 0.56 mm, which indicates that only a very thin layer of the bed participates in the sediment entrainment process. This finding in turn implies that there is little interaction between the ~ 2 m thick muck in the lake and the water column, because even a BSSL with an unlikely high concentration of, say, 700 kg L^{-1} would correspond to a less than 10 mm thick bed layer.

The persistence of a "constant" BSSL in the lake may be explained on a time-mean basis in terms of the wind kinetic energy required to raise the potential energy of a layer of suspension to the height of the BSSL. Quite simply, wind energy is expended in expanding a 0.56 mm thick bottom layer with a dry density of 100 kg m^{-3} to a 0.80 m high BSSL with SSC of 70 mg L^{-1}. To provide a mechanistic explanation of this phenomenon, Vinzon and Mehta (1998) used the steady state form of the turbulent kinetic energy balance to obtain the equilibrium height H_e of the BSSL as a function of wave properties. The semi-theoretical equation was shown to be

$$H_e = 0.65 \left(\frac{(a_b{}^3 k_s)^{3/2}}{T^3 \dfrac{\rho_s - \rho_w}{\rho_w} g w_o \varphi_v} \right)^{1/4}$$

(8)

where ρ_s is the particle density, g is the acceleration due to gravity and $\varphi_v = C/\rho_s$ is the mean volumetric concentration of the suspended solids.

For estimating H_e using Eq. (8) we will choose the following nominal values: $a_b =$ 0.015 m based on Eq. (5b) with $H = 0.07$ m, $T = 1.4$ s and $h = 1.6$ m, $k_s = 0.1$ m (instead of the secular value of 0.01 m, in order to account for local bottom variability), $\rho_s = 1,700$ kg m^{-3}, $\rho_w = 1,000$ kg m^{-3}, $w_o = 1.15 \times 10^{-4}$ m s^{-1}, and $\varphi_v = 70/(1700 \times 1000) = 0.041 \times 10^{-3}$. This yields $H_e = 0.68$ m, which is within the measured range.

An important basis of Eq. (8) is that it does not embody the concept of a threshold for resuspension (in terms of the bed shear strength τ_s). To account for the presence of suspended sediment in the lake water column at low discharges (≤ 1 m^3 s^{-1}) and wind speeds (≤ 2 m s^{-1}), it would be necessary to reduce the shear strength to less than 0.002 Pa, the combined current-wave shear stress under these conditions. Such low shear

strength implies that the sediment in suspension under these conditions consists mostly of organic material with density close to water. At high discharges and wind speeds one can expect heavier particles to be brought into suspension. If so, the composition of sediment leaving Prairie Creek must vary with the hydraulic conditions in the lake, and that, in general, the material would be finer than that at the lake bottom. Qualitative observations of sediment in suspension appear to be consistent with this inference.

To entrain organic matter at very low discharges and wind speeds must require a hydrodynamic forcing mechanism at the bottom. Conceivably it is provided by a relative motion between water and the bottom sediment layer susceptible to movement. Evidence for such likelihood is found in Fig. 16, in which the vertical amplitude of the fluid (muck) acceleration recorded 0.2 m below the muck surface is plotted against wind speed. As the accelerometer data showed numerous discrepancies, only a limited number of data points are included. Despite this limitation, we observe a clear trend of increasing amplitude with wind speed, with 3.2 m s^{-1} as a threshold wind speed marking the onset of muck heave. Heave would suggest a relative motion at the muck surface and associated shear stress that would be absent over a hard bed. In laboratory wave-flume experiments Maa and Mehta (1987) observed interfacial waves at the soft mud surface, and estimated the contribution to bed shear stress from the relative motion between the mud surface and the boundary layer in water. They found that this contribution can be a significant fraction of the bed shear stress estimated from hard bed analysis.

Pore pressure data given in Table 5 corroborate muck movement recorded by the accelerometer. Unfortunately, pore pressure values showed substantial scatter, with little likelihood of obtaining a reliable correlation with wind speed (Jain et al., 2005).

16

NUTRIENT LOADS

Nutrient data collected at the platform included concentrations of dissolved organic nitrogen, dissolved organic phosphorus, nitrate-nitrite, ammonia, particulate nitrogen, particulate phosphorus, soluble reactive phosphorus, total dissolved nitrogen, total dissolved phosphorus, total Kjeldahl nitrogen and total phosphorus. None of these species, which were obtained during six sets of data collection over the study period, showed any dependence on the wind speed. This was so, in part, because water sampling using the auto-samplers was carried out at 1 to 3 hour intervals over 24 to 72 hr periods. Diurnal variation in nutrient concentrations was apparently too weak to be detected during these periods. At the same time, the sampling duration was insufficiently long for identifying frontal oscillations in concentrations.

Nutrient concentrations were also measured daily by SJRWMD in the streams and the lake (at mid-depth) over different periods: Hatchet Creek and Bee Tree Creek during 2003-2004, Little Hatchet Creek during 1998-2004, Prairie Creek during and 1997-2004 and Newnans Lake in 2004. These synoptic data are evidently important for assessing a nutrient budget for the lake. A plot of the dissolved and total load of total Kjeldahl nitrogen (TKN) against discharge, which is typical of all the species and all the stations, is shown in Fig. 17 for Hatchet Creek. There is little evidence of any significant contribution from the particulate load, presumably because of low SSC in the system as a whole. The same conclusion can be drawn for all the species (Jain et al., 2005). As in Fig. 11, linear data fit implies a constant TKN concentration. Thus, given the discharge time-series for the inflows and outflow and assuming a linear relationship between the load and discharge, it was straightforward to calculate the cumulative mass of TKN over any

desired period, and thereby establish a mass balance for the lake. Similar analysis for carried out for all other species (Jain et al., 2005).

In Table 8, besides TKN we have calculated masses of total phosphorus (TP) and dissolved phosphorus (DP), ammonia (NH_4) and nitrate-nitrite (NOx) for the 10-day "non-event" calibration period in February. The results are given in terms of cumulative inflow mass m_I, cumulative outflow mass m_O (Fig. 18), the difference m_I-m_O and the ratio $(m_I$-$m_O)/m_I$. Judging from the last two quantities we conclude that TP and DP were in near balance, but TKN, NH_4 and NOx were exported from the lake. Since an insignificantly thin bottom sediment layer exchanges material with the water column, it appears that over the 10-day period the lake supplied nitrogen from sources not accounted for by the two inflow creeks or the lake bottom. The most likely source is the accumulated nitrogen in the lake water itself, presumably coupled with diffusion from bottom sediment and the effects of bioturbation.

In Table 9 we have presented calculations for the 7-day hurricane period in September. Due to high discharges the cumulative masses are up to two orders of magnitude higher than in February. However, at the end of this event, with the exception of TKN, supply from the inflow creeks exceeded outflow from Prairie Creek. In other words, the lake sequestered incoming nutrients represented *by m_I-m_O.*

CONCLUDING COMMENTS

From the hydraulic point of view, Newnans Lake may be thought of as a shallow and wide open channel in which transport of sediment from the creeks is modulated by wind effects in the lake. Light weight, organic-rich fine sediment particles dominate the

suspended matter, and SSC response to wind occurs over a wide frequency band whose range is determined by the combined forcing due to wind effects and stream discharges.

On a time-mean basis, wind kinetic energy maintains sediment as a Benthic Suspended Sediment Layer with a mean height of about 0.80 m and a mean SSC of about 70 mg L^{-1}. The sediment mass in this suspension is equivalent to less than 1 mm thick bed layer, which suggests that there is little interaction between the ~ 2 m thick muck in the lake and the water column.

Nutrient mass balance analysis is simplified because dissolved nutrient loads are close or nearly equal to total loads, with minor to negligible contributions from the low-concentration particulate matter. Mass balances for phosphorus and nitrogen indicate periods on the order of days over which the lake acts both as a net exporter and a net importer of these nutrients.

ACKNOWLEDGMENT

REFERENCES

Dean, R. G., and Dalrymple, R. A., 1991. *Water Wave Mechanics for Engineers and Scientists.* World Scientific, Singapore.

Gowland, J. E., Mehta, A. J., Stuck, J. D., John, C. V. and Parchure, T. M., 2005. Organic-rich fine sediments in Florida part II: Resuspension in a lake. *Estuarine and Coastal Fine Sediment Dynamics*, J. P.-Y. Maa, L. P. Sanford and D. H. Schoellhamer eds., Elsevier, Amsterdam, 162-183.

Hamrick, J. M., 1992. A three dimensional environmental fluid dynamics computer code: Theoretical and computational aspects. *Special Report No 317*. Applied Marine Science and Ocean Engineering, Virginia Institute of Marine Science, Gloucester Point, VA.

Hamrick, J. M., 1996. User's manual for environmental fluid dynamics computer code. *Special Report No 331*. Applied Marine Science and Ocean Engineering, Virginia Institute of Marine Science, Gloucester Point, VA.

Hamrick, J. M., 2000. Theoretical and computational aspects of sediment transport in the EFDC model. *Technical Memorandum*, Tetra Tech, Inc., Fairfax, VA.

Jain, M., Mehta, A. J., Hayter, E. J., and McDougal, W. G., 2005. A study of sediment and nutrient loading in Newnans Lake, Florida. *Report UFL/COEL-2005/002*, Coastal and Oceanographic Engineering Program, Department of Civil and Coastal Engineering, University of Florida, Gainesville.

Maa P.-Y. and Mehta A. J., 1987. Mud erosion by waves: a laboratory study. *Continental Shelf Research*, 7(11/12), 1269-1284.

Mehta, A. J., 1991. Understanding fluid mud in a dynamic environment. *Geo-Marine Letters*, 11, 113-118.

Park, K., A. Y. Kuo, J. Shen, and J. M. Hamrick, 2001. A three-dimensional hydrodynamic-eutrophication model (HEM3D): description of water quality and sediment processes submodels. *Special Report* 327, The College of William and Mary, Virginia Institute of Marine Science, Gloucester Point, VA.

Richards, A., 2003. Sea breeze genesis - A missing factor. *MSc thesis*, School of Mathematics Meteorology and Physics, University of Reading, UK.

Ross M. A. and Mehta A. J., 1989. On the mechanics of lutoclines and fluid mud. *Journal of Coastal Research*, SI 5, 51-61.

Soulsby, R., L., Hamm, L., Klopman, G., Myrhaug, D., Simons, R. R., and Thomas, G. P., 1993. Wave-current interaction within and outside the bottom boundary layer. *Coastal Engineering*, 21, 41-69.

Table 1 Instruments deployed at the platform

Property	Instrument make	Model no.	Freq. of bursting (Hz)
Wind	RM Young anemometer	05103	-
Air temperature	Analog Devices gauge	AC 2626	-
Water temperature	Analog Devices gauge	AC 2626	-
Current	Sontek acoustic current meter	Field ADV	10
Air pressure	Trans-metrics gauge	B020	-
Total (H_2O) press.	Trans-metrics gauge	P215L	10
Pore (H_2O) press.	Druck gauge	PDCR-81	10
TSS	Sea Point sensors (OBS)	-	10
Fluid acceleration	Analog Devices accelerometer	ADXL 202	10
Data logging	Campbell Scientific logger	CR23X	-
Light	Carmanah light	501	-
Data transmission	Airlink Comm. modem	Redwing CDMA	-

Table 2 Coefficients for stress calculation

Coefficient	Value
a_1	-0.06
a_2	1.70
a_3	-0.29
a_4	0.29
M_1	0.67
M_2	-0.29
M_3	0.09
M_4	0.42
N_1	0.75
N_2	-0.27
N_3	0.11
N_4	-0.02
I	0.80

Table 3 Lake physical parameters

Month	Water temperature (^oC)	Rainfall (mm)	Mean wind speed [a] ($m\ s^{-1}$)	Maximum wind speed [b] ($m\ s^{-1}$)	Prairie Cr. discharge ($m^3\ s^{-1}$)
January	16.9	1.3	3.2	10.3	0.64
February	17.5	4.9	4.1	11.4	0.89
March	22.0	1.6	3.7	9.4	1.24
April	24.4	1.0	3.7	12.6	0.92
May	29.3	0.4	3.3	11.1	0.50
June	31.0	5.2	2.6	12.9	0.26
July	32.6	3.2	2.5	8.9	0.21
August	31.9	75.0	3.0	10.5	0.42

[a] Monthly average of ½-hourly (2-min mean) values.
[b] Peak value in a month.

Table 4 Wave parameters at the platform

Month	Maximum wave height [a] (m)	Maximum modal wave period [b] (s)	Max. horz. wave orbital current ampl. (m s^{-1})	Max. vert. wave orbital current ampl. (m s^{-1})	Max. vert. wave orbital acc. ampl. (m s^{-2})
January	0.14	1.2	0.17	0.13	0.45
February	0.14	1.3	0.18	0.13	0.41
March	0.16	1.3	0.20	0.13	1.71
April	0.16	1.4	0.20	0.12	1.58
May	0.14	1.3	0.20	0.15	0.4
June	0.28	1.2	0.47	0.39	0.41
July	0.16	1.2	0.21	0.14	-
August	0.18	1.3	0.23	0.16	2.37

[a] Significant wave height is defined as four times the root-mean-square of surface elevation.
[b] Modal wave period is defined as the period corresponding to the frequency at the wave spectral peak.

Table 5 Current, SSC and pore pressure at the platform

Month	Mean current (mm s^{-1})	SSC-1[a] (mg L^{-1})	SSC-2[b] (mg L^{-1})	SSC-3[c] (mg L^{-1})	Depth-mean SSC (mg L^{-1})	Maximum muck pore pressure (kPa)
January	2.6	7.1	20	176	68	50
February	4.2	8.8	17	155	60	95
March	2.8	12.4	39	254	102	140
April	3.3	12.0	46	239	99	158
May	1.4	9.6	52	230	97	268
June	2.5	8.8	110	119	79	326
July	2.8	6.1	111	116	78	-
August	0.3	3.4	117	-	-	281

[a] OBS-1 elevation 1.8 m above bed; [b] OBS-2 1.4 m; [c] OBS-3 1.1 m.

Table 6 SSC characteristics related to wind speed

Month	OBS elev.[a] (m)	$\bar{C}$			$\hat{C}$		$\hat{C}/\bar{C}$
		$\bar{a}$	$\bar{b}$	@ 4 m s^{-1} (mg L^{-1})	$\hat{a}$	@ 0.5 m s^{-1} (mg L^{-1})	
February	1.8	0.31	7.0	8.2	0.67	0.3	0.04
	1.4	0.25	15.5	16.5	0.77	0.4	0.02
	1.1	0.08	148	162	36.3	18.1	0.11
May	1.8	0.16	8.8	9.4	2.0	1.0	0.11
	1.1	8.2	193	226	10.7	5.4	0.02

[a] With respect to bed surface.

Table 7 Measured and simulated time-mean SSC at the platform

OBS	SSC		Error (%)
	Measured (mg L^{-1})	Simulated (mg L^{-1})	
1	8	7	-13
2	16	20	+25
3	150	113	-25

Table 8 Cumulative nutrient masses during the 10-day non-event period

Species	Inflow (m_I) (t)	Outflow (m_O) (t)	Diff. (m_I-m_O) (t)	(m_I-m_O)/m_I
TP	0.05	0.11	-0.06	-1.2
DP	0.05	0.03	+0.02	+0.4
TKN	0.47	1.76	-1.29	-2.7
NH$_4$	0.02	0.19	-0.17	-8.5
NOx	0.02	0.09	-0.07	-3.5

Table 9 Cumulative nutrient masses during the 7-day hurricane period

Species	Inflow (m_I) (t)	Outflow (m_O) (t)	Diff. (m_I-m_O) (t)	(m_I-m_O)/m_I
TP	2.6	0.8	-1.8	-0.7
DP	2.6	0.2	-2.4	-0.9
TKN	30.5	13.9	+16.6	+0.5
NH$_4$	1.19	1.49	-0.3	-0.3
NOx	0.45	0.75	-0.3	-0.7
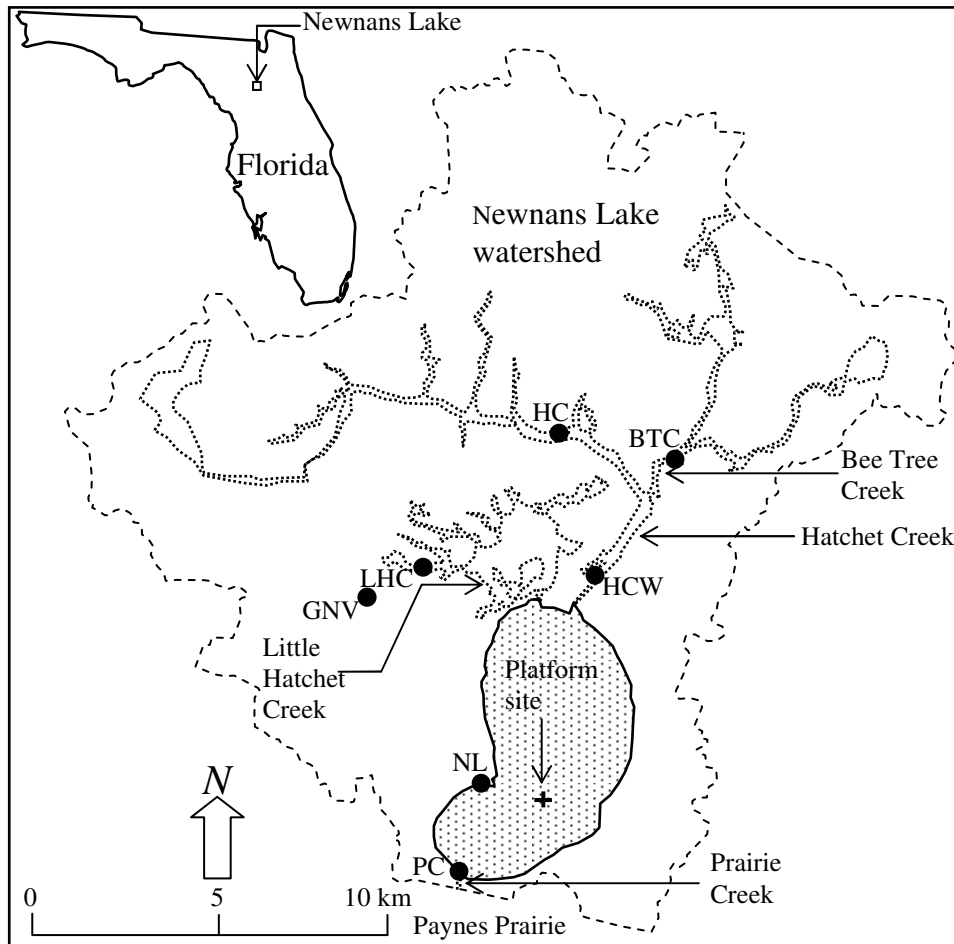
Figure 1 Newnans Lake and watershed in north-central Florida.
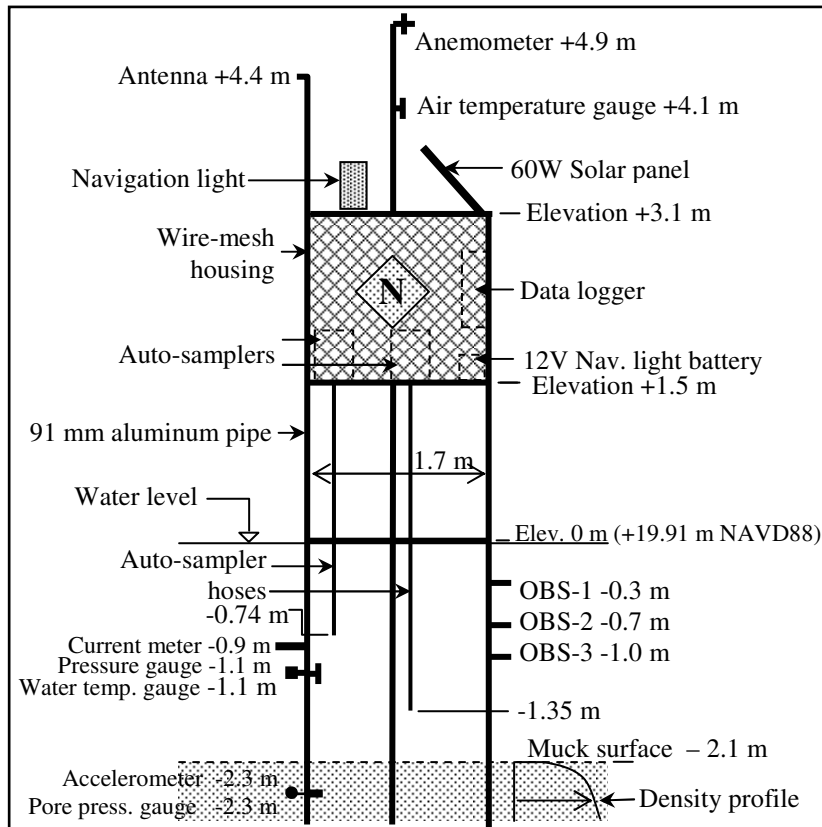
Figure 2 Field platform and instrumentation.
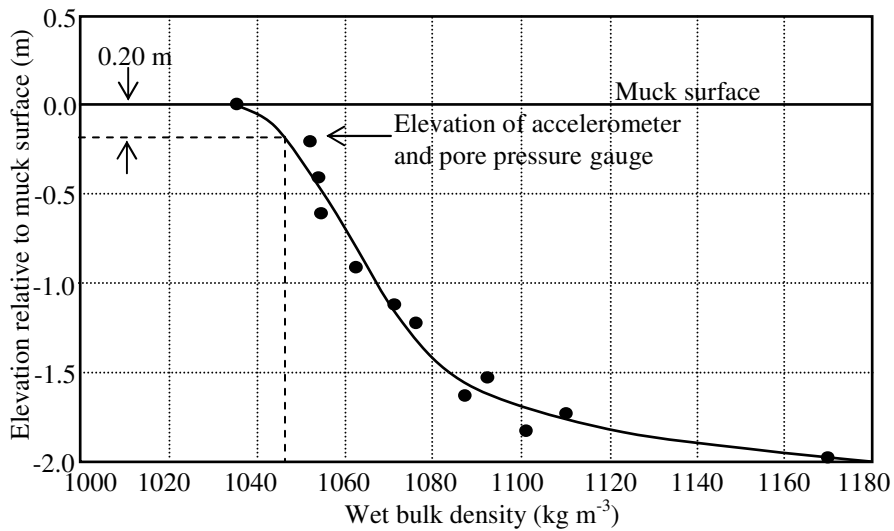
Figure 3 Bottom muck density profile at the platform site.
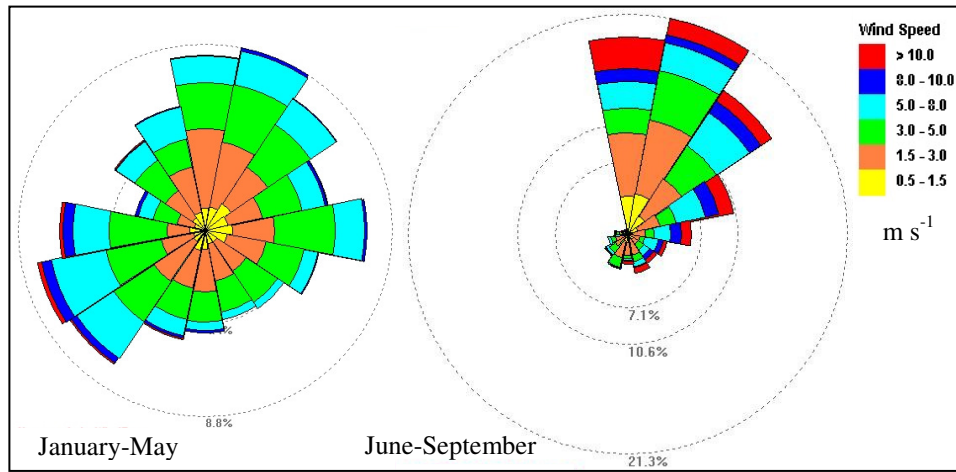
Figure 4 Wind roses for January-May and June-September 2004.
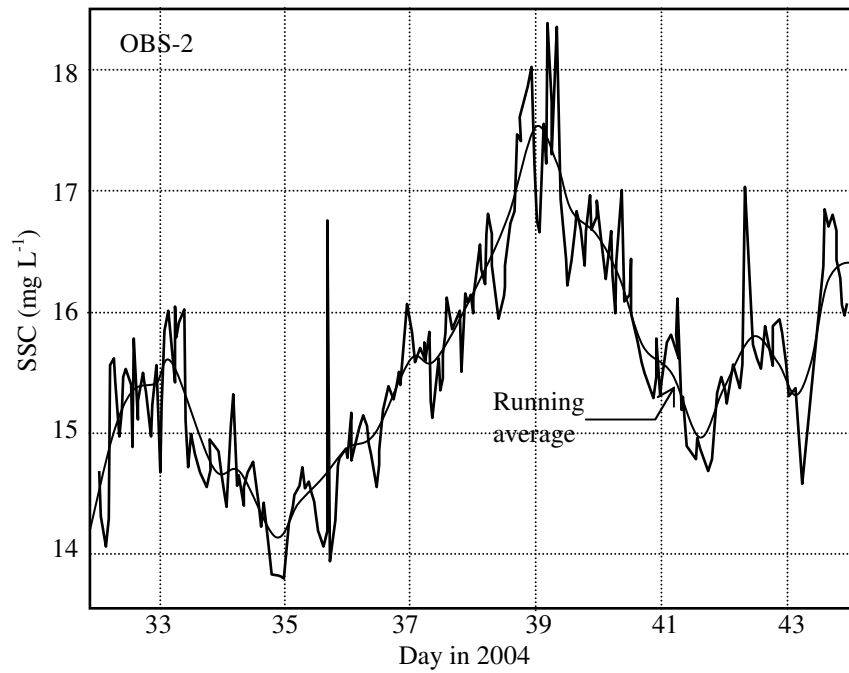
Figure 5 Sample time-series of variation of SSC measured by OBS-2.
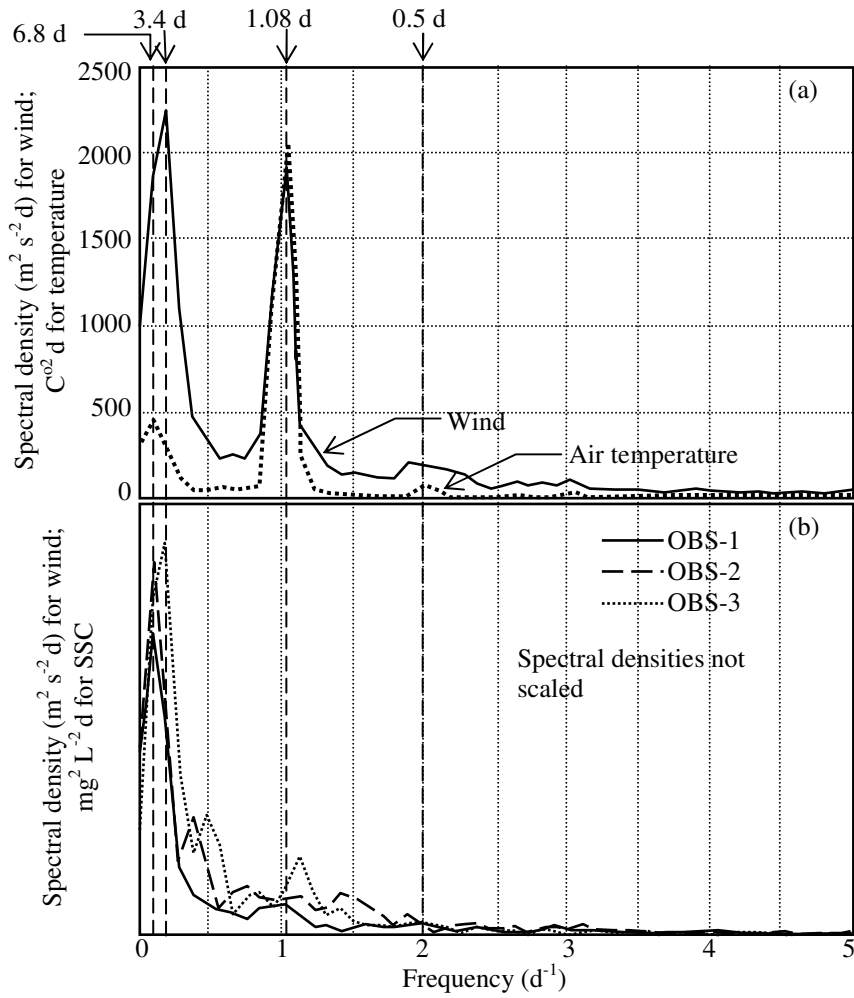
Figure 6 Wind, air temperature and SSC spectra.
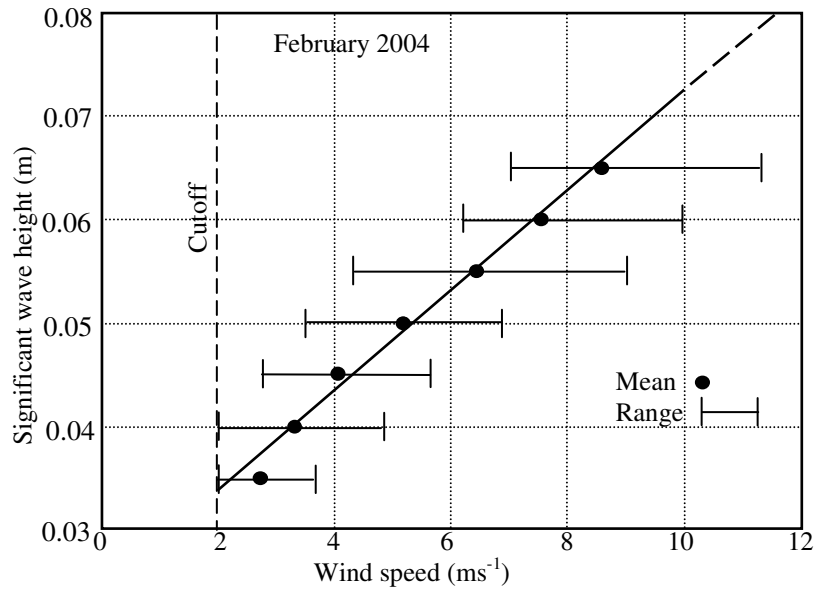
Figure 7 Variation of significant wave height with wind speed.
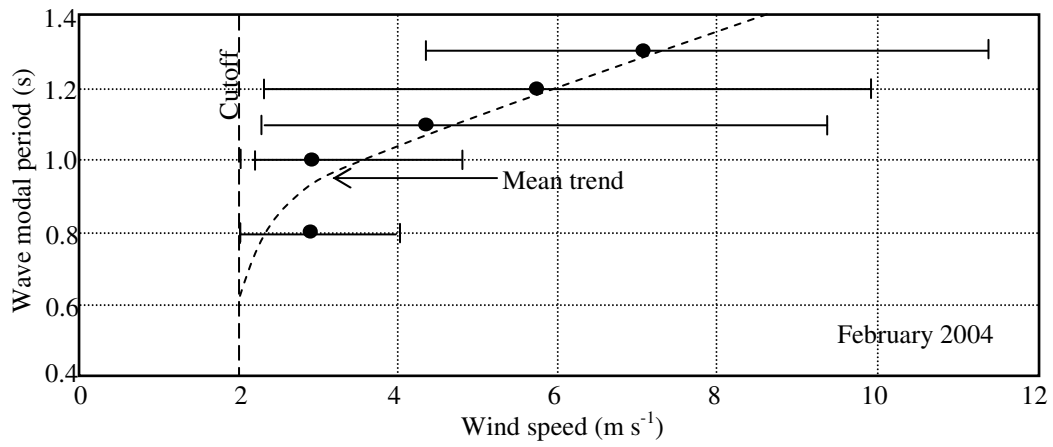
Figure 8 Variation of wave modal period with wind speed.
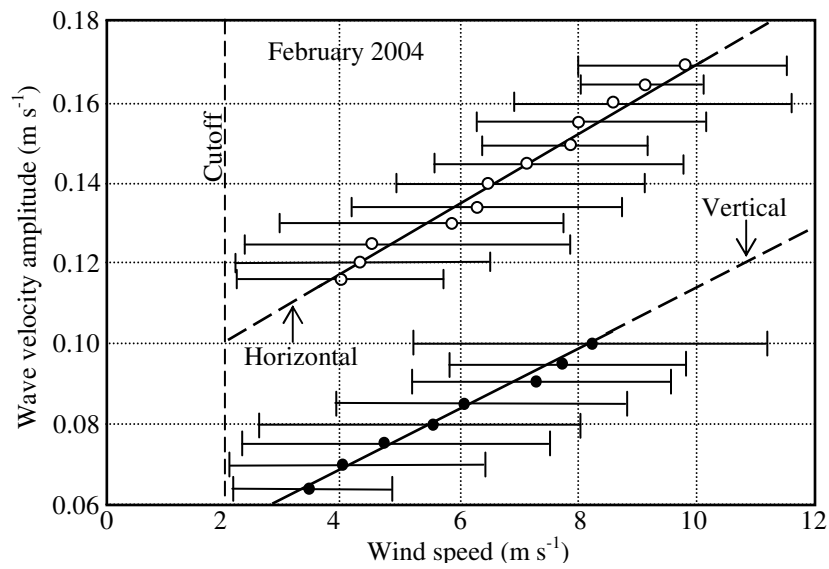
Figure 9 Variation of wave orbital velocity amplitudes with wind speed.
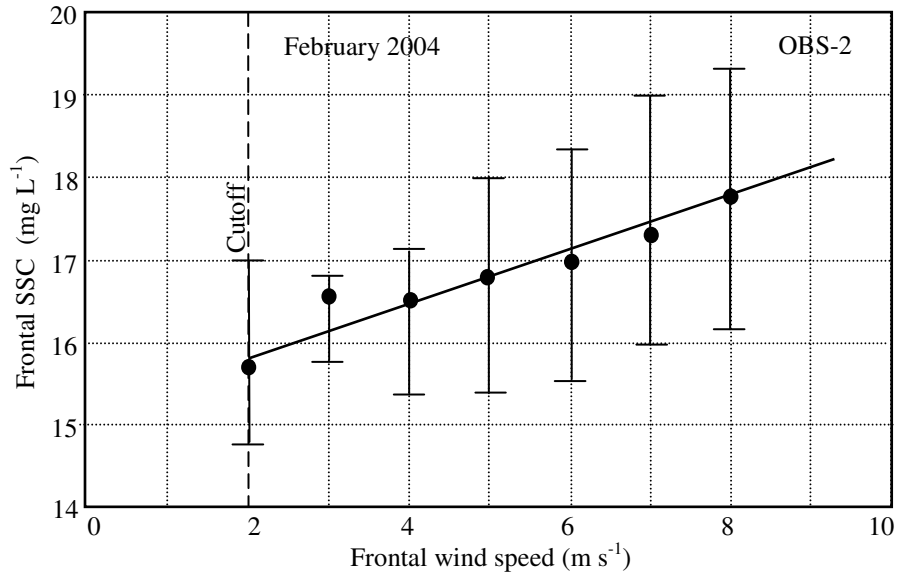
Figure 10a Variation of frontal SSC ($\overline{C}$) with frontal wind speed ($\overline{U}$) at OBS-2.
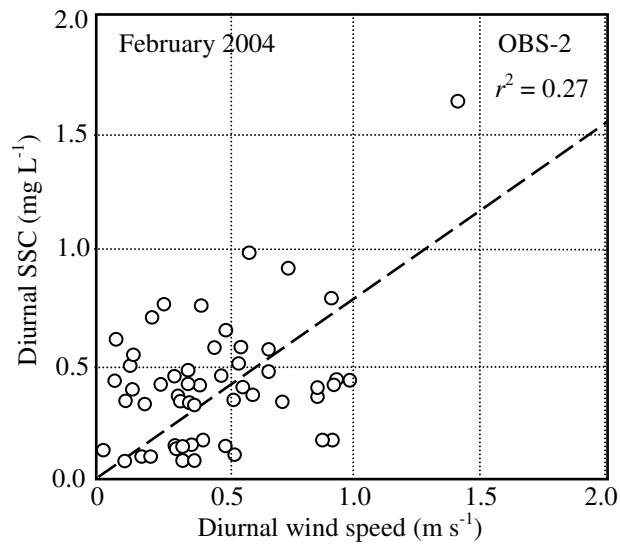
Figure 10b Variation of diurnal SSC ($\hat{C}$) with diurnal wind speed ($\hat{U}$) at OBS-2.
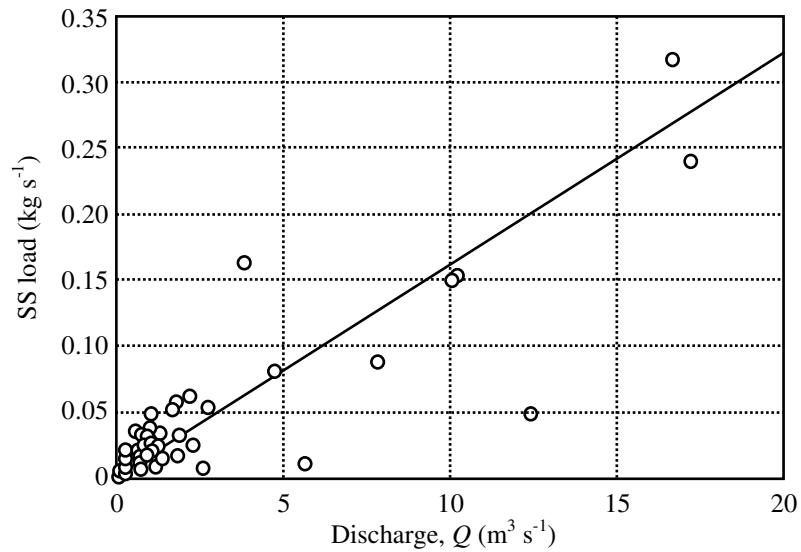
Figure 11 Variation of SSC load with discharge in Prairie Creek.
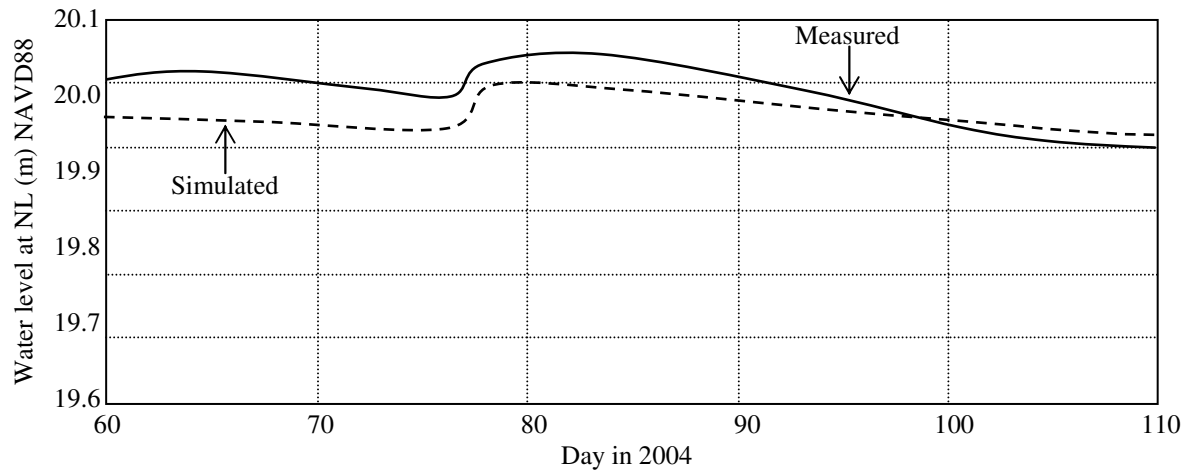
Figure 12 Comparison of measured and simulated water levels in the lake.
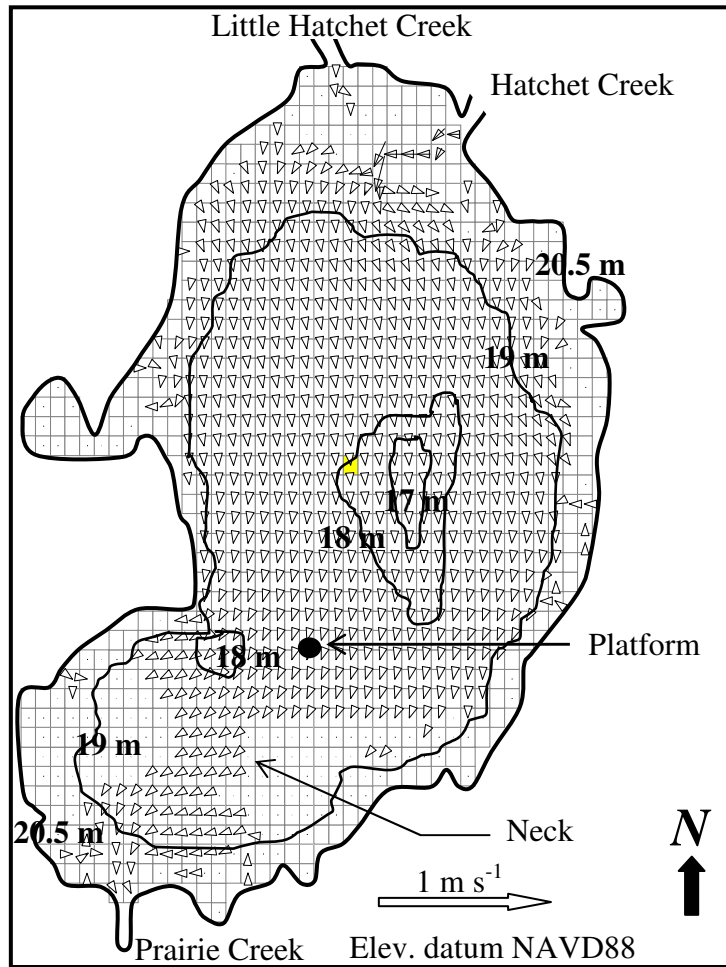
Figure 13 Simulated surface velocity vectors. Selected depth contours are shown.
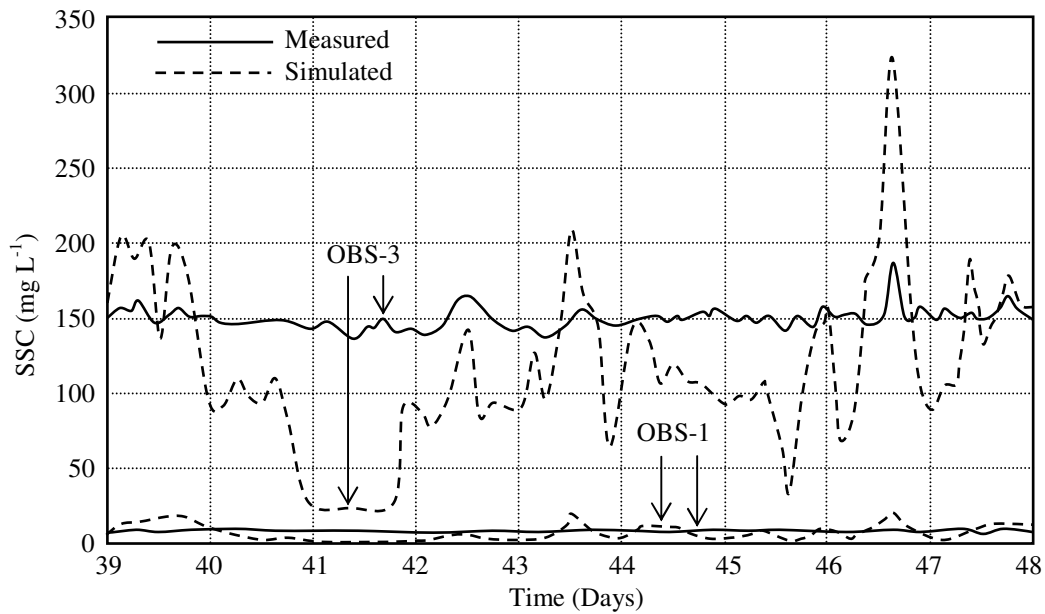
Figure 14 Measured and simulated SSC time-series for OBS-1 and OBS-3.
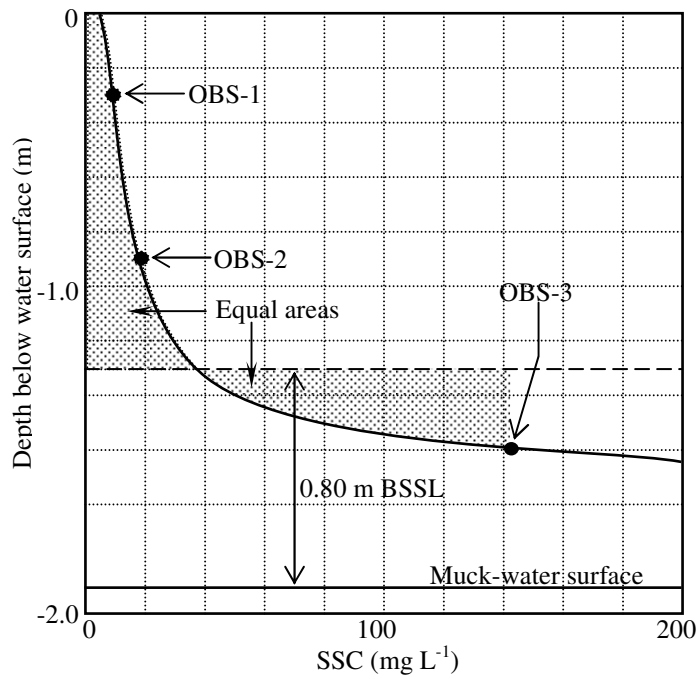
Figure 15 Typical SSC profile and estimation of BSSL height.
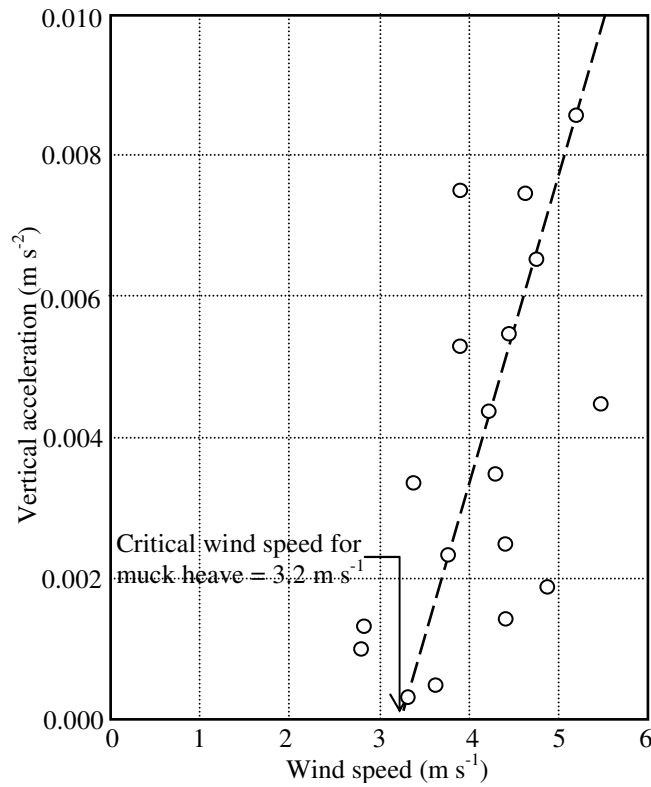
Figure 16 Vertical acceleration in mud versus wind speed during February, March and May.
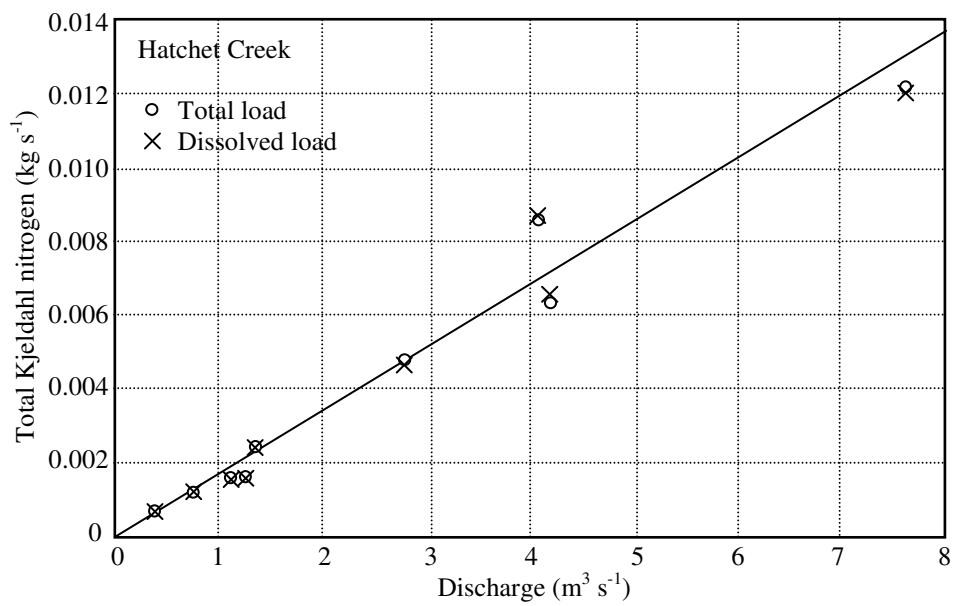
Figure 17 Total load of TKN versus discharge in Hatchet Creek.
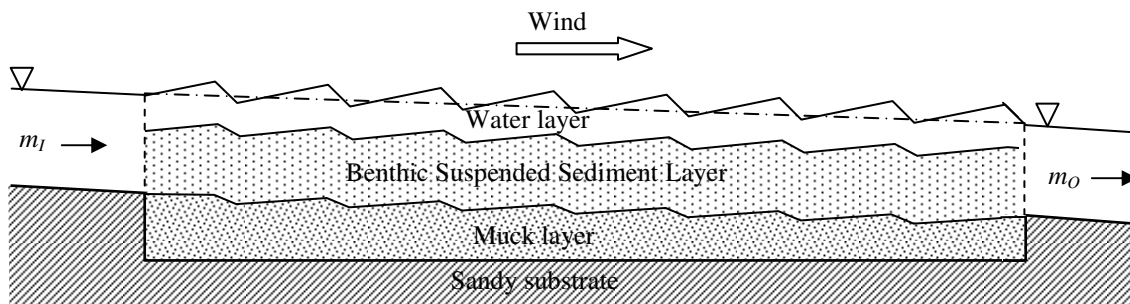
Figure 18 Inflow and outflow nutrient masses.

Space-based monitoring of wetland surface flow

Basic Information

Title:	Space-based monitoring of wetland surface flow
Project Number:	2004FL76G
Start Date:	9/1/2004
End Date:	8/31/2007
Funding Source:	104G
Congressional District:	18
Research Category:	Not Applicable
Focus Category:	Wetlands, Surface Water, Hydrology
Descriptors:	
Principal Investigators:	Shimon Wdowinski

Publication

1. Wdowinski, S., F. Amelung, T. Dixon, F. Miralles-Wilhelm, and R. Sonenshein, Space-based detection of surface water level changes in South Florida, submitted to Remote Sensing for Environment, 2005.
2. Wdowinski, S., F. Amelung, F. Miralles-Wilhelm, T. Dixon, and R. Carande, Space-based hydrology of the Everglades wetland, South Florida, First National Conference on Ecosystem restoration, Abstract Volume, p. 466, 2004. 44.
3. Wdowinski, S., F. Amelung, and T. Dixon, Towards operational monitoring of wetland water levels using InSAR: Applications for the Everglades Restoration Project, Eos Trans. AGU, 85(47), Fall Meet. Suppl., Abstract H23E-1169, 2004.
4. Wdowinski, S., F. Amelung and T. Dixon, S. Kim, B. Osmanoglu, M. Kartal, D. Harding, The Everglades wetlands as a laboratory for testing and calibrating the CRYOSAT hydrological applications.
5. Osmanoglu, M., D. Kartal, S. Wdowinski and T. Dixon, Altitude accuracy improvement by using a new radar altimeter simulator for ENVISAT data, 1st CRYOSAT meeting, 2005.
6. Kim, S., S. Wdowinski, F. Amelung, and T. Dixon, C-Band Interferometric SAR Measurements of Water Level Change in the Wetlands: Examples from Florida and Louisiana, IGARSS meeting proceedings, 2005.
7. Wdowinski, S., F. Amelung, and T. Dixon, Space-Based hydrology of the Everglades Wetlands, South Florida, Society of Wetland Scientists, 26th Annual Meeting, Final program and abstracts, 125, 2005.
8. Wdowinski, S., F. Amelung, T. Dixon, S. Kim, B. Osmanoglu, M. Kartal, and D. Harding, The Everglades wetlands as a laboratory for testing and calibrating space-geodetic hydrological

technologies, Eos Trans. AGU, 86(18), Fall Meet. Suppl., Abstract G23A-04, 2005.

9. Kim, S., S. Wdowinski, F. Amelung and T. Dixon, Wetlands Application of Interferometric SAR Measurements: examples from Florida and Louisiana, Eos Trans. AGU, 86(18), Fall Meet. Suppl., Abstract G23A-03, 2005.
10. Bieler, B.M, R. Garcia-Martinez, F. Miralles-Wilhelm, and S. Wdowinski, Modeling Water Flow in the Everglades Wetlands Using Interferometric Synthetic Aperture Radar (InSAR)Observations, Eos Trans. AGU, 86(18), Fall Meet. Suppl., Abstract G23A-05, 2005.
11. Kim, S, A. Ferretti, F. Novali, S. Wdowinski, F. Amelung, T.H. Dixon, R.K. Dokka, and B. Rabus, Observation of Subsidence in New Orleans Using Permanent Scatterers, Eos Trans. AGU, 86(18), Fall Meet. Suppl., Abstract G43A-04, 2005.

Progress Report

Space-based monitoring of wetland surface flow

PI: Dr. Shimon Wdowinski

Division of Marine Geology and Geophysics, Rosenstiel School of Marine and Atmospheric Science, University of Miami

Progress has been obtained in the following four categories:

1. Data acquisition

We continue acquiring C-band SAR data, mainly over the Everglades wetlands, but also over other wetlands. Our main source of data for Everglades is RADARSAT-1, which has a repeat orbit of 24 days. Using our Alaska SAR Facility (ASF) data project, we set 6 Data Acquisition Requests (DAR) that automatically acquire every repeat orbit. As a result, we get 6 new acquisitions within every 24 days, half using fine beam (7 m pixel resolution) and the other half with standard beam (15 m resolution). Due to a new agreement between ASF and CSTARS (University of Miami), since October we downlink the new acquisitions at CSTARS at no cost! So, we are getting high quality data at no cost and in real time.

We also continue ordering and obtaining ENVISAT data using our ESA CAT-1 data projects. We collect ENVISAT data over the Everglades, Louisiana coastal wetlands, Chesapeake Bay, Pantanal (Brazil), and Mauritania, and Okavango Delta (Botswana). The ENVISAT repeat orbit is 35 days, which found to be problematic in some cases. Nevertheless, we continue collecting the data and evaluating its importance.

2. Data processing and results

We have continued processing both archive and current data. We completed processing the archived L-band JERS-1 data of south Florida. The data covers the time span of 1993-1996 and shows very interesting features. The results of this study are summarized in a manuscript that was submitted to RSE and is currently in the review process. We processed some of the archived C-band ERS-1/2 data of the Everglades. However, we still need to re-process this data set with our improved processing scheme. We also process the current C-band data of the Everglades and other wetlands. Some preliminary results of these processing were presented at the ESA (European Space Agency) sponsored Fringe meting in November 2005. We also presented at that meeting a comprehensive analysis of the Everglades data, using all data type (JERS-1, ERS-1/2, ENVISAT, and RADARSAT-1). This study is in an advanced stage and will be submitted soon for publication.

3. Flow models

Our systematic analysis of all available data has shown that the fine beam (7 m pixel resolution) RADARSAT-1 (C-band) data produce best results. Therefore we routinely

obtain such data using our ASF data project (see section 1). For some of the orbit we collected already a year-long data, with 24 day time span between acquisitions. Routine processing of the data enables us to produce interferogram time-series showing water level changes in some sections of the Everglades. One of our focus area is Water Conservation Area 1 (WCA-1), which its unique hydrological conditions generate very interesting fringe patterns. This series of interferograms are now being used by a MS student, B.M. Bieler, to constrain a high spatial-resolution flow model of WCA-1, using a Finite Element technique. The model equations are solved using an explicit finite element scheme that facilitates parallelization and incorporation of adaptive methods, and is well suited for short term simulations. In order to construct the model's geometry, we use a dynamic mesh generator, which can produce variable resolution meshes. Such meshes are considered essential to obtain the required spatial resolution in the highly variable environment of the Everglades. Preliminary modeling results show very good fit to some of the observations, but not all. The model needs further improvements, which will be conducted in the next few months.

Information Transfer Program

During FY 2005, the Florida WRRC actively promoted the transfer of the results of water-resources research to water-resource groups in Florida. The target audience was the scientific and technical community who address Floridas water problems on a professional basis. Specific activities that were part of this task included maintaining an updated mailing list with email addresses and a web-based home page. The email list and home page were used to provide timely information about research proposal deadlines, conference announcements and calls for papers, and other water-related activities. The home page describes ongoing research at the WRRC and lists research reports and publications that are available. Also, the home page is used to list research reports and publications that are available through the WRRC and elsewhere, and it provides links to other water-resource organizations and agencies, including the five water management districts in Florida and the USGS. The WRRC continues to maintain a library of technical reports that have been published in past years by the WRRC. Copies of these reports can be checked out by researchers. Also, copies of reports are distributed upon request with a nominal charge make to cover the cost of reproduction and mailing. As newer reports become available, electronic versions of these reports will be made available for distribution by downloading from the WRRC home page. Financial support was provided for publishing research results in refereed scientific and technical journals and conference proceedings.

Information Transfer

Basic Information

Title:	Information Transfer
Project Number:	2005FL99B
Start Date:	3/1/2005
End Date:	2/28/2006
Funding Source:	104B
Congressional District:	6th
Research Category:	Not Applicable
Focus Category:	None, None, None
Descriptors:	
Principal Investigators:	Kirk Hatfield, Mark Newman

Publication

1. Newman, M., K. Hatfield, J. Hayworth, P.S.C. Rao, and T. Stauffer. Inverse characterization of NAPL source zones. Environmental Science and Technology. 2006, (In Review).
2. Campbell, T.J., K. Hatfield, H. Klammler, M.D. Annable, P.S.C Rao. Magnitude and directional measures of water and Cr(VI) fluxes by passive flux meter. Environmental Science and Technology. 2006, (In Review).
3. Klammler, H K. Hatfield, M. Annable, E. Agyei, B. Parker, J. Cherry, and P.S.C. Rao. General analytical treatment of the flow field relevant for passive fluxmeter interpretation. Water Resour. Res. 2005, (In review).
4. Bhat, S., K. Hatfield, J. M. Jacobs, R. R. Lowrance, R. G. Williams, and K. R. Reddy. Prediction of Nitrogen Leaching from Freshly Fallen Leaves: Application of the Riparian Ecosystem Management Model (ReMM), Journal of Hydrology. 2005, (In Review).
5. Brown, C. J., and S. Sutterfield, J. R., Hendel, P. J. Kwiatkowsiki, J. Mirecki, K. Hatfield. The Comprehensive everglades restoration program ASR pilot projects: Plan development, J. Water Resour. Planning and Management. 2005, (In review).
6. Bhat, S., J. M. Jacobs, K. Hatfield, and W. Graham. Hydrologic indices of watershed scale military impacts of Fort Benning, Ga. Journal of Hydrology. 2004, (In Review).
7. Mohamed, M K. Hatfield, and A. E. Hassan. Monte Carlo evaluation of contaminant biodegradation in heterogeneous aquifers, Advances in Water Resources. 2005, (In Press).
8. Sedighi, A., H. Klammler, C. Brown, and K. Hatfield. A semi-analytical model for predicting water quality from an aquifer storage recovery system, Journal of Hydrology. 2005, (In Press).
9. Perminova, I.V., A.N. Kovalenko, P. Schmitt-Kopplin, K. Hatfield, N. Hertkorn, E.Y. Belyaeva, V.S. Petrosyan. Design of quinoid-enriched humic materials with enhanced redox properties,

Environmental Science and Technology. 39 (2), 2005, 8518-8524.

10. Bhat, S., J. M. Jacobs, K. Hatfield, and J. Prenger. Relationships between Water Chemistry and Land Use in Military Affected Watersheds in Fort Benning, Georgia, Ecological Indicators, 6(2), 2006, 458-466.

11. Agyei, E. and K. Hatfield. Enhancing gradient-based parameter estimation with an evolutionary approach. Journal of Hydrology. 316 (1-4), 2005, 266-280.

12. Newman, M., K. Hatfield, J. Hayworth, P.S.C. Rao, and T. Stauffer. A hybrid method for inverse characterization of subsurface contaminant flux, Journal of Contaminant Hydrology, 81(1-4), 2005, 34-62.

13. Mohamed, M and K. Hatfield. 2005. Modeling Microbial-mediated reduction in batch reactors, Chemosphere, 59(8), 1207-1217.

14. Clark, C.J., K. Hatfield, M. D. Annable, P. Gupta, and T. Chirenje. 2005, Estimation of arsenic contamination in groundwater by the passive flux meters, Journal of Environmental Forensics, Vol 6, 2005, 77-82.

Student Support

Student Support					
Category	**Section 104 Base Grant**	**Section 104 NCGP Award**	**NIWR-USGS Internship**	**Supplemental Awards**	**Total**
Undergraduate	1	0	0	0	1
Masters	4	0	0	0	4
Ph.D.	4	0	0	0	4
Post-Doc.	3	0	0	0	3
Total	12	0	0	0	12

Notable Awards and Achievements

For the upcoming year (FY 2006) the Florida Water Resources Research Center has been restructured with the goal of maximizing the amount of graduate student funding available to the state of Florida under the provisions of section 104 of the Water Resources Research Act of 1984 (Public Law 98-242). Agreements have been established with three of Floridas Universities (Florida State University, University of South Florida, and the University of Florida) and four state agencies (South Florida Water Management District, Southwest Florida Water Management District, St. Johns River Water Management District, and the Florida Geological Survey) that will support the work of 10 Ph.D. students for FY2006. These agreements will be funded with support from the United States Geological Survey ($92,335) along with matching funds from the collaborating universities and state agencies ($220,481) to provide $312,816 in total support for water resources related research in FY2006.

The supported research projects will consider a wide range of water resource related issues while maintaining focus on topics specific to Florida. These topics include investigating the geochemical processes that control the mobilization of arsenic during aquifer storage recovery (ASR), comparing widely used procedures by which radar- and gauge-derived rainfall are optimally combined for water management and regulatory decisions, investigating the measurement of evapotranspiration, recharge, and runoff in shallow water table environments characteristic of the Gulf of Mexico coastal plain, studying the measurement of erosion around and flow through hydraulic structures and culverts, and developing software for quantifying the impacts of saltwater up-coning and well field pumping.

The Florida Water Resources Research Center has also provided support for continued development of innovative methods for measuring the movement or flux of groundwater and groundwater contaminants using a recently patented passive flux meter. Portions of this research were funded by the Natural and Accelerated Bioremediation Research (NABR) program, Biological and Environmental Research (BER), U.S. Department of Energy, the FloridaWater Resources Center under a grant from the U.S. Department of Interior, and the Environmental Security Technology Certification (ESTCP) program, U.S. Department of Defense (DoD).

Publications from Prior Projects

1. 2004FL57B ("Sensitivity of the Hydroperiod of Forested Wetlands to Alterations in Topographic Attributes and Land Use") - Articles in Refereed Scientific Journals - Nachabe, M. H 2006. Spatially Distributed Versus Lumped Parameter Models: A proposed Equivalence between the TOPMODEL and SCS Curve Number Method. Journal of the American Water Resources Association, 42(1):225-235.
2. 2004FL57B ("Sensitivity of the Hydroperiod of Forested Wetlands to Alterations in Topographic Attributes and Land Use") - Articles in Refereed Scientific Journals - Said, A., M. Nachabe, M. Ross, and J. Vomacka 2005. Estimating Specific Yield Using Continuous Soil Moisture Monitoring, ASCE Journal of Irrigation and Drainage Engineering, vol. 131, no.6.
3. 2004FL57B ("Sensitivity of the Hydroperiod of Forested Wetlands to Alterations in Topographic Attributes and Land Use") - Articles in Refereed Scientific Journals - Nachabe, M. H., N. Shah, M. Ross, and J. Vomacka 2005 . Evapotranspiration of Two Vegetation Covers in Humid Shallow Water Table Environment. Soil Science Society of America Journal, 69:492-499.
4. 2004FL57B ("Sensitivity of the Hydroperiod of Forested Wetlands to Alterations in Topographic Attributes and Land Use") - Articles in Refereed Scientific Journals - Nachabe, M. H., C. Masek, and J. Obeysekera 2004. Observations and Modeling of Profile Soil Water Storage above a Shallow Water Table. Soil Science society of America Journal, Vol. 68, No. 3.
5. 2004FL57B ("Sensitivity of the Hydroperiod of Forested Wetlands to Alterations in Topographic Attributes and Land Use") - Articles in Refereed Scientific Journals - Hernandez, T., M. Nachabe, M. Ross, and J. Obeysekera 2004. Runoff from Variable Source Areas in Humid, Shallow Water Table Environments. Journal of the American Water Resource Association, vol. 39, no. 1, pp.75-85.
6. 2004FL57B ("Sensitivity of the Hydroperiod of Forested Wetlands to Alterations in Topographic Attributes and Land Use") - Articles in Refereed Scientific Journals - DeSilva, M., M. H. Nachabe, J. Simunek, and R. Carnahan 2006. Simulating Root Water Uptake from a Heterogeneous Vegetation Cover using Finite Element Modeling. (In review).
7. 2004FL57B ("Sensitivity of the Hydroperiod of Forested Wetlands to Alterations in Topographic Attributes and Land Use") - Articles in Refereed Scientific Journals - DeSilva, M. and M. H. Nachabe 2006. Influence of Changes in Land Use and Topographic Attributes on Hydrology of Shallow Water Table Environments. In preparation.